Journal of Medicinal Chemistry

PURDUE UNIVERSITY

Subscriber access provided by Purdue University Libraries

Article

Discovery and Structure Activity Relationship (SAR) of a Series of Ethanolamine-Based Direct-Acting Agonists of Sphingosine-1-Phosphate (S1P1)

John L Gilmore, James E Sheppeck, Scott H. Watterson, Lauren Haque, Parag Mukhopadhyay, Andrew Joseph Tebben, Michael A. Galella, Ding Ren Shen, Melissa Yarde, Mary Ellen Cvijic, Virna Borowski, Kathleen M. Gillooly, Tracy Taylor, Kim W. McIntyre, Bethanne Warrack, Paul C. Levesque, Julia P. Li, Georgia Cornelius, Celia J. D´Arienzo, Anthony M. Marino, Praveen V. Balimane, Luisa Salter-Cid, Joel C. Barrish, William J. Pitts, Percy H Carter, Jenny Xie, and Alaric J. Dyckman

J. Med. Chem., **Just Accepted Manuscript** • DOI: 10.1021/acs.jmedchem.6b00373 • Publication Date (Web): 16 Jun 2016

Just Accepted

ACS Publications

Journal of Medicinal Chemistry is published by the American Chemical Society. 1155 Sixteenth Street N.W., Washington, DC 20036

	Development, Discovery Biology Dyckman, Alaric; Bristol-Myers Squibb, Discovery Chemistry

Discovery and Structure Activity Relationship (SAR) of a Series of Ethanolamine-Based Direct-Acting Agonists of Sphingosine-1-Phosphate ($S1P_1$)

John L. Gilmore, James E. Sheppeck II, Scott H. Watterson, Lauren Haque, Parag Mukhopadhyay, Andrew J. Tebben, Michael A. Galella, Ding Ren Shen, Melissa Yarde, Mary Ellen Cvijic, Virna Borowski, Kathleen Gillooly, Tracy Taylor, Kim W. McIntyre, Bethanne Warrack, Paul C. Levesque, Julia P. Li, Georgia Cornelius, Celia D'Arienzo, Anthony Marino, Praveen Balimane, Luisa Salter-Cid, Joel C. Barrish, William J. Pitts, Percy H. Carter, Jenny Xie, Alaric J. Dyckman.*

Bristol-Myers Squibb Research and Development, P.O Box 4000, Princeton, NJ 08543

ABSTRACT: Sphingosine-1-phosphate (S1P) is a bioactive sphingolipid metabolite that regulates a multitude of physiological processes such as lymphocyte trafficking, cardiac function, vascular development, and inflammation. Because of the ability of $S1P_1$ receptor agonists to suppress lymphocyte egress, they have great potential as therapeutic agents in a variety of autoimmune diseases. In this article, the discovery of selective, direct acting $S1P_1$ agonists utilizing an ethanolamine scaffold containing a terminal carboxylic acid is described. Potent $S1P_1$ agonists such as compounds **18a** and **19a** which have greater than 1000-fold

selectivity over $S1P_3$ are described. These compounds efficiently reduce blood lymphocyte counts in rats through 24 hours after single doses of 1 mpk and 0.3 mpk respectively. Pharmacodynamic properties of both compounds are discussed. Compound **19a** was further studied in two preclinical models of disease, exhibiting good efficacy in both the rat adjuvant arthritis model (AA) and the mouse experimental autoimmune encephalomyelitis model (EAE).

INTRODUCTION

Sphingosine-1-phosphate (S1P) is a bioactive sphingolipid metabolite formed from the conversion of ceramide by ceramidase followed by subsequent phosphorylation by sphingosine kinases.[1,2] S1P regulates a multitude of physiological processes including lymphocyte trafficking, cardiac function, vascular development, and inflammation. These biological functions are mediated through the interaction of S1P with five G-protein coupled receptors known as $S1P_{1\text{-}5}$.[3] Agonism of the $S1P_1$ receptor has been shown to block lymphocyte trafficking from the thymus and secondary lymph nodes resulting in immunosuppression.[4,5] One theory explains this effect of $S1P_1$ agonism by postulating that it causes a tightening of the lymphatic endothelial cell junctions which prevents lymphocytes from leaving the lymphoid tissue.[6,7] Another theory postulates that the activation of the S1P receptor by synthetic agonists leads to prolonged receptor internalization causing a desensitization of the cell toward the S1P concentration gradient.[6,8] This S1P concentration gradient between blood plasma and lymph is proposed to be the driving force for the lymphocytes to exit the lymph nodes. These S1P receptor agonists are thus behaving as functional antagonists preventing the egress of lymphocytes from the thymus and lymph nodes. Because of the ability of $S1P_1$ receptor agonists to suppress lymphocyte egress, they have great potential as therapeutic agents in a variety of

autoimmune diseases such as rheumatoid arthritis, lupus, multiple sclerosis, and inflammatory bowel disease.

Fingolimod (**1**) was approved for the treatment of relapsing/remitting multiple sclerosis.[9] Compound **1** (fingolimod) is a non-selective S1P receptor agonist which is dosed as a prodrug and subsequently phosphorylated (**1-P**) *in vivo,* much like S1P.[10] Compound **1** is an effective immunosuppressant; however, it has been to shown to cause a transient, dose-dependent decrease of heart rate in clinical studies.[11] This undesired effect as well as several others were thought to be caused by agonism of the $S1P_3$ receptor.[12] Studies in rodents have shown that $S1P_3$ activation leads to many undesired effects such as heart rate reduction, vasoconstriction, bronchoconstriction, and blood pressure increase.[13,14] Since $S1P_3$ receptor agonism is not required to prevent lymphocyte egress, many research groups have been working toward the discovery of potent $S1P_1$ agonists which are $S1P_3$ sparing in hopes of finding compounds that will not have these undesired effects.[15,16] However, recent clinical studies with S1P agonists with selectivity for $S1P_1$ over $S1P_3$ have suggested that in humans, heart rate effects are controlled, at least in part, by the $S1P_1$ receptor.[17,18] Nonetheless, since $S1P_3$ receptor agonism does not contribute to the efficacy, finding selective compounds remained an emphasis for our research efforts.

Our initial research efforts in the identification of improved $S1P_1$ compounds were aimed at direct acting agonists rather than the pro-drug class exemplified by **1**. A direct-acting agonist avoids the complication of two overlapping structure activity relationships since it does not require an *in vivo* phosphorylation step to produce the active species. Another advantage of the direct-acting compounds is the potential to reduce the *in vivo* half-life of the compounds. The

human half-life of **1** is 6-9 days which resulted in an extended pharmacodynamic effect upon drug discontinuation.[19]

The general motif of these direct-acting $S1P_1$ agonists is to have a lipophilic tail and a polar headgroup joined by a rigid aryl or heteroaryl linker. Others have replaced the phosphate polar headgroup with a carboxylic acid to achieve very potent and selective $S1P_1$ agonists.[15,19] More specifically, an azetidine carboxylic acid group has been effectively utilized as a replacement for the phosphate (**2**),[14,20] and we have previously explored its use with a variety of lipophilic tails and linkers.[21] Use of the azetidine carboxylic acid group led to the discovery of **4** (BMS-520) which was our first development candidate.[21] In our continued research efforts, we sought to discover new polar headgroups that would produce compounds with the requisite activity, selectivity, and pharmacokinetic profile. Herein, we describe our medicinal chemistry efforts which resulted in the discovery of novel polar headgroups based on an ethanolamine scaffold containing a terminal carboxylic acid group.

RESULTS AND DISCUSSION

Our search began by utilizing a readily accessible lipophilic tail (3-phenyl-4-propylisoxazole) previously discovered in our laboratories as contained in compound **3** (Figure 1). The routes employed to synthesize our ethanolamine scaffolds are shown in Scheme 1. The first step was to build the isoxazole carboxylic acid by heating pent-1-ynylbenzene and diethyl 2-nitromalonate in a stainless steel pressure bomb at 160°C for 18 hours to form ethyl 5-phenyl-4-propylisoxazole-3-carboxylate. Next, the ethyl ester was hydrolyzed with aqueous base and the resulting acid (**5**) was converted to an acid fluoride with cyanuric fluoride. This acid fluoride was coupled with N'-hydroxy-4-vinylbenzimidamide (**6**) which was prepared by heating 4-

vinylbenzonitrile with hydroxylamine in 2-propanol. This coupled intermediate was subsequently cyclized to form the central oxadiazole ring by heating at 70 ^{o}C in acetonitrile to afford **7**. Compound **7** was converted to epoxide **8** using m-CPBA. From the epoxide, two methods were employed to obtain the final products. The first method was to open the epoxide with phthalimide followed by treatment with hydrazine to form ethanolamine **9**. The terminal amine of **9** was then coupled with an appropriately substituted alkyl halide containing a terminal ester. Deprotection of the terminal ester by treatment with TFA afforded the final product (**11a**). The second method employed was to open epoxide **8** by treatment with bromotriethylsilane at -78 ^{o}C in THF to yield **10**. Reaction of the resulting bromo group with an appropriately substituted amine using DBU or tetrabutylammonium hydroxide as a base afforded the desired compounds after purification (**11b-m**). All of the propylisoxazole analogs (**9, 11a-m**) described above were synthesized as a mixture of isomers with regard to the hydroxyl moiety of the ethanolamine framework. Many of these compounds exhibited promising activity and selectivity and Table 1 shows the key results of these ethanolamine based compounds.

Interestingly, **9**, which has no terminal carboxylic acid group to mimic the phosphate moiety, had excellent activity in the $S1P_1$ binding assay with an IC_{50} of 1.5 nM and had modest activity in the functional $S1P_1$ GTPγS assay with an EC_{50} of 64 nM. This compound also exhibited some selectivity against $S1P_3$ (~34 fold). To increase the activity in the functional assay, a linear alkyl chain with a terminal acid was appended off of this amino group (**11a**). This compound was a sub-nanomolar binder in the $S1P_1$ binding assay and the addition of the terminal carboxylic acid did indeed increase the $S1P_1$ GTPγS activity giving an EC_{50} of 38 nM. Next, a variety of pyrrolidine, piperidine, cyclopentyl and piperazine compounds containing a carboxylic acid were synthesized (**11b-j**). These compounds all have the carboxylic acid

positioned two carbons from the ethanolamine nitrogen as compounds with the carboxylic acid one carbon away had reduced activity (data not shown). The pyrrolidine-3-carboxylic acid compound (**11b**) was potent in the $S1P_1$ binding assay with an IC_{50} of 0.69 nM; however, its functional activity was only modest ($S1P_1$ GTPγS EC_{50} of 61 nM). Compound **11c**, which contains a 2-pyrrolidine acetic acid, and **11d**, which contains a 2-piperidine acetic acid, both demonstrated poor activity in both the binding and functional assays. We next examined piperidine compounds with the carboxylic acid moiety directly attached to the 3-position of the piperidine (**11e-f**). Compound **11e** which has the *S* stereochemistry at this position proved to be optimal with an EC_{50} of 6.9 nM in the $S1P_1$ GTPγS assay. The corresponding diastereomeric mixture (**11f)** was greater than 20 times less potent. Compounds **11g-h** are cyclopentyl derivatives in which the amine and carboxylic acid are exocyclic and have a cis configuration. Both isomers had excellent $S1P_1$ binding with **11g** being roughly three times more potent than **11h**. This more potent compound was analyzed in the $S1P_1$ GTPγS functional assay providing an EC_{50} of 27 nM. Replacing the 3-carboxylic acid of the piperidine with a hydroxyl group (**11i**) proved to be detrimental for both binding and functional activity, and converting the piperidine to a piperazine while maintaining the carboxylic acid in the 3 position (**11j**) also reduced both the $S1P_1$ binding and GTPγS activity. Placing a methylene spacer in between the piperidine and carboxylic acid in the 3 position, however, provided compounds with potent functional activity (**11k-m**). After preparing the compounds with *R* (**11l**) and *S* (**11m**) stereochemistry at the acid center, **11l**, was the most potent compound in this series with a GTPγS activity of 3.9 nM and a 300 fold selectivity over $S1P_3$.

Select compounds were chosen from Table 1 to be evaluated in an *in vivo* rat blood lymphocyte reduction (BLR) pharmacodynamic/pharmacokinetic (PD/PK) assay to assess their

ability to reduce peripheral blood lymphocyte counts in Lewis rats. The linear alkyl analog (**11a**) and the two most potent compounds from the piperidine series (**11e** and **11l**) were all evaluated in this assay and the results are shown in Table 2. At an oral dose of 30 mpk, compound **11a** reduced the peripheral lymphocyte counts by 74% when checked 4 hours post administration. By the 24 hour time point, the lymphocyte counts had returned to normal levels. Compound **11e** was dosed at 10 mpk and exhibited a 77% reduction in the peripheral lymphocyte counts. Again, by the 24 hour timepoint, the lymphocyte counts had returned to normal levels. Compound **11l**, which was the most potent of the compounds evaluated in Table 1, was dosed at 3 mpk. At 4 hours post-dose, this compound exhibited an 81% reduction in the peripheral lymphocyte count and at 24 hours showed a 25% reduction. The return of lymphocyte counts to baseline for these analogs was consistent with the reduction in compound plasma concentrations from 4 hours to 24 hours. These results prompted us to evaluate these new polar headgroups with our optimal lipophilic tails.

We combined the lipophilic tail (3-phenyl-4-(trifluoromethyl)isoxazole) from **4** with the preferred fragments found here (**11e** and **11l**). The same relative stereochemistry for both these piperidine headgroups was found to be optimal and this stereochemistry was kept constant for these new analogs. Again, the initial SAR studies of these analogs was performed on a mixture of isomers with regard to the hydroxyl moiety of the ethanolamine framework. The azetidine-3-carboxylic acid moiety, which has been utilized by a number of groups with great success, albeit on different scaffolds, was also incorporated here as part of the ethanolamine framework. Our synthesis (Scheme 2) began by coupling the commercially available (2-bromoacetyl)benzonitrile with tert-butyl azetidine-3-carboxylate, (*S*)-ethyl piperidine-3-carboxylate and (*R*)-ethyl 2-(piperidin-3-yl)acetate. These compounds were then reduced using sodium borohydride in

ethanol to give the corresponding alcohols (**12,14,15**). To install the lipophilic tail piece of **4**, the nitrile group was first heated with hydroxylamine and sodium bicarbonate in isopropanol and then coupled with 3-phenyl-4-(trifluoromethyl)isoxazole-5-carbonyl fluoride. Treatment of this intermediate with 1M TBAF in THF cyclized the coupled product to form the central oxadiazole ring. Finally, deprotection of the terminal ester either by aqueous acid hydrolysis or treatment with TFA afforded the final products (**13,16,17**).

Table 3 contains the binding and functional activities of **13**, **16**, and **17** as well as their ability to reduce lymphocyte counts in an *in vivo* BLR PK/PD assay. Compound **13**, which incorporates the azetidine-3-carboxylic acid and the lipophilic tail from **4**, provided a compound with an $S1P_1$ binding IC_{50} of 5.8 nM and demonstated impressive $S1P_1$ functional activity and selectivity against $S1P_3$ (EC_{50} = 7.8 nM, ~1500 fold selectivity). In the BLR PK/PD assay, **13** reduced the lymphocyte count by 70% at a dose of 3 mpk when measured at the 24 hour timepoint. The (*S*)-piperidine-3-carboxylic acid headgroup with the lipophilic tail of **4** (**16**) also gave a compound with impressive binding and functional activity ($S1P_1$ binding IC_{50} = 0.47 nM; $S1P_1$ GTPγS EC_{50} = 7.8±3.5 nM), and this compound also gave greater than 1500 fold selectivity over $S1P_3$. In the BLR PK/PD assay, **16** exhibited an 81% reduction in lymphocytes at a dose of 3 mpk at the 24 hour timepoint. As in the propylisoxazole series, the (*R*)-piperidin-3-yl)acetic acid ethanolamine headgroup was the most potent compound (**17**). Compound **17** had an $S1P_1$ GTPγS EC_{50} of 4.2±1.0 and displayed ~1000 fold selectivity over $S1P_3$. When dosed at 1 mpk in the BLR PK/PD assay, **17** reduced the lymphocyte count by 75% when checked after 24 hours. These compounds all showed a marked improvement over the initial propylisoxazole series as that series showed little to no significant reduction of lymphocytes after 24 hours at a dose of 3-10 mpk.

Next, the stereochemistry at the hydroxyl position for the piperidine analogs (**16,17**) was analyzed to determine if there was a preference at this chiral center as well. Compounds **14** and **15** were again reduced using sodium borohydride in ethanol to give the corresponding alcohols (Scheme 2). These alcohols were then separated under chiral SFC conditions to provide each isomer (**14a, 14b, 15a, 15b**). The stereochemistry of both centers of **14a** was unambiguously determined by small molecule x-ray analysis.[22] The stereochemistry of **15a** was later determined through a synthesis using a chiral reducing agent of known induction.[23] Each compound was then carried through the next steps as previously described to afford the two piperidine carboxylic acid isomers **18a** and **18b** and the two piperidine acetic acid isomers **19a** and **19b**.

The functional activities of the homochiral optimal polar headgroups combined with the lipophilic tailpiece of **4** are shown in Table 4. In the piperidine carboxylic acid series, the stereochemistry at the acid center was set as *S* since this proved to more active in the previous series, and the stereochemistry at the alcohol center was studied with both the *R* and *S* configuration. The compound with the *1S,2S* stereochemistry (**18a**) was more active in the $S1P_1$ GTPγS assay with an EC_{50} of 3.5±1.5 nM as compared to 30±9 nM for the *1S,2R* isomer (**18b**). In the piperidine acetic acid series, the same relative stereochemistry at the alcohol center proved to be the more active isomer and **19a** was the most active in the series with an EC_{50} of 1.2±0.52 nM in the GTPγS assay. These compounds all show excellent selectivity against $S1P_3$ (>1000 fold). The two more active isomers were also tested against $S1P_4$ and $S1P_5$. Compound **18a** had EC_{50}'s of around 1 nM for both these receptors while **19a** was slightly more active with EC_{50}'s of roughly 0.5 nM against both.

After determining the most favorable stereochemistry at both the hydroxyl centers (*S* for both series) and carboxylic acid centers (*S* for the piperidine carboxylic acid and *R* for the

piperidine acetic acid), other lipophilic tails were synthesized with these two novel polar headgroups using the methods shown in Scheme 2. Table 5 shows the results of selected compounds in both the $S1P_1$ and $S1P_3$ functional assays as well as results from *in vivo* BLR PK/PD to determine lymphocyte reductions at the 24 hour timepoint. The first two compounds are with the lipophilic tail from **4** and their in vitro activities were previously discussed. At an oral dose of 0.3 mpk, both of these analogs were very effective at reducing the peripheral lymphocyte count with **18a** showing 54% reduction and **19a** showing 80% reduction after 24 hours. Changing the phenyl group on the oxazole to a pyridyl group (**20a-b**), gave a compound with similar potency in the $S1P_1$ GTPgS assay and was even more selective against $S1P_3$. There was, however, a slight reduction in efficacy in the BLR PK/PD assay. Reversing the N and O to form the alternate isoxazole isomer resulted in roughly equal potency in the functional assays (**21a-b**). In the BLR PK/PD assay, the alternate isoxazole isomer with the piperidine carboxylic acid (**21a**) was somewhat less effective exhibiting a 13% reduction of lymphocytes at 1 mpk. However, the alternate isoxazole isomer with the piperidine acetic acid (**21b**) was equally effective as its counterpart (**19a**) with a 76% reduction at a dose of 0.3 mpk. Next, we examined replacing the phenyl group with alkyl and cycloalkyl derivatives and limited these to the piperidine acetic acid polar headgroup (**22-23**). In general, the compounds with an alkyl substituent were sufficiently active in the $S1P_1$ GTPγS functional assay but were much less effective in the BLR PK/PD assay. The best compound from these analogs is **23** which had a 49% reduction in lymphocytes. While we had several lipophilic tails which showed promise with these ethanolamine-based polar headgroups, we decided to further analyze **18a** and **19a** both *in vitro* and *in vivo* to assess whether they would be candidates for further progression.

To understand the specific interactions with $S1P_1$, compound **19a** was docked into the crystal structure of $S1P_1$ in complex with **24** (ML056)[24] (Figure 2). The model suggests that the aromatic tail is buried deeply within the transmembrane bundle in a cavity formed between TM2, TM3, TM5 and TM6. The polar headpiece is predicted to be oriented toward the extracellular side of the receptor forming hydrogen bonding interactions with residues at the top of TM1 and TM7 as well as the N-terminus. Two salt bridges are predicted to be present with residues on TM7: the terminal acetic acid moiety and R292 and the piperidine nitrogen and E294. Additional hydrogen bonds are predicted between the acetic acid-T48 and the hydroxyl group-E294/K34. The strong interactions with the hydroxyl group are consistent with the SAR showing it to be a critical group.[25] Although **24** and **19a** putatively fill the same hydrophobic pocket, the polar interactions predicted by the model are different than those observed to the amino phosphonate moiety in **24** (Figure 2b). The amino group is more deeply buried within the transmembrane region, forming a hydrogen bond with N101. The phosphonate is in a salt bridge with K34 and hydrogen bonded with Y29. Compound **19a** is predicted to share an interaction with K34, but the remaining polar interactions are on the protein surface.

Figure 3 shows the results of a BLR PK/PD study to investigate the dose response for compounds **18a** and **19a**. The compounds were assessed at three doses and the blood lymphocyte count was determined at 4 and 24 hours. Compound **18a** was dosed orally at 1, 0.3, and 0.1 mpk. At 1mpk, **18a** showed maximal lymphocyte reduction at both the 4 hr and 24 hr timepoints and a clear dose dependency was observed. Using the exposure data from this experiment, the EC_{50} and ED_{50} for **18a** were estimated to be 19 nM and 0.6 mpk respectively at the 24 hour timepoints. Being more potent, **19a** was dosed at 0.03, 0.1 and 0.3 mpk. Again, a clear dose response was observed with the highest dose giving maximal lymphocyte reduction

for this assay at both the 4 and 24 hour timepoints. For **19a**, the exposure data at the 24 hour timepoint gave an EC_{50} of 19 nM with an ED_{50} of 0.1 mpk.

The pharmacodynamic properties of **18a** and **19a** are shown in Table 6. These compounds are both highly bound to plasma proteins in mouse, rat, monkey, dog and human (>98.7%), and *in vitro* liver microsomes studies indicated the metabolic clearance of **18a** and **19a** was very low in all species (>98% remaining). Consistent with the low in vitro clearance, both compounds had low systemic clearance *in vivo* ranging from 0.1 to 1.7 mL/mg/kg. Compound **18a** had consistently good absolute bioavailability in all species with F% ranging from 62-90%. The $T_{1/2}$ from species to species was somewhat inconsistent with a low of 9 hours in rat to high of 33 hours in cynomolgus monkey. Additionally, the peak to trough ratio was inconsistent with mouse and monkey having ratio of 1.7 while rat and dog had ratios of 6.7 and 11.3 respectively. In contrast, compound **19a** exhibited very consistent PK across all species. The $T_{1/2}$ ranged from 23-28 hours and the peak to trough was equally consistent ranging from 1.3 to 2.8. The absolute bioavailabilities were very good with **19a** exhibiting slightly better results than **18a** in rat, monkey and dog.

The ability of **19a** to drive receptor internalization was investigated using CHO cells transfected with human $S1P_1$ fused with GFP. In this assay, **19a** acted as a full agonist inducing $S1P_1$ internalization with an EC_{50} of 5.0 ±4.6 nM (n=35). Compound **19a** was further characterized for off-target as well as genotoxic potential (Table 7). It was screened for its selectivity against a large panel of receptors, transporters and kinases and no appreciable activities were detected (data not shown) and **19a** was negative in the Ames assay. Some activity was detected in the ion channel assays. In cardiac repolarization assays (hERG patch clamp), **19a** exhibited an IC_{50} of 4.1 μM. Given the high level of protein binding observed with

this compound, we surmised it would still have a low cardiac liability. As **19a** exhibited consistent pharmacodynamic behavior across multiple species and possessed an acceptable liability profile, we chose to study it in animal models.

Figure 4 and Figure 5 show compound **19a** in two pre-clinical models of disease. Figure 4 shows the results of a rat adjuvant induced arthritis model (rat AA), a model for human rheumatoid arthritis[26], and the data shown demonstrates the suppressive effects of orally administered **19a** over the 21-day study. In rats dosed with vehicle only, there was an increase in paw volume beginning at day 11, and this swelling reached a maximum level at day 15 (1.5 mL increase). Rats given **19a** at doses of 0.06, 0.2 and 1.0 mpk exhibited a dose dependent reduction in the amount of paw edema. In fact, in the groups treated with 0.2 and 1 mpk of **19a**, there was no paw volume increase observed throughout the duration of the study. The rats dosed at 0.06 mpk had paw edema beginning at day 13 and at day 20 had roughly half the amount of swelling as the vehicle group. From this study, the compound was determined to have an ED_{50} of 0.05 mpk in the rat AA model.

We also evaluated the suppressive effect of **19a** on experimental autoimmune encephalomyelitis (EAE). EAE has been used as a preclinical animal model for proof of concept studies for multiple sclerosis therapy. The graph in Figure 5 demonstrates the effects of orally administered **19a** in this EAE study. Vehicle-administered mice began to show clinical signs from Day 10, and thereafter an acute increase of the EAE score was observed reaching maximal level on Day 18. Compound **19a** was given at once-daily doses of 0.01, 0.1 and 1 mpk with p.o. dosing initiated at the time of immunization. All doses were efficacious lowering the EAE clinical scores taken from Day 12 until the completion of the study when compared to the vehicle treated group.

In summary, we have discovered selective, direct acting $S1P_1$ agonists utilizing a novel polar headgroup consisting of an ethanolamine scaffold with a terminal carboxylic acid. This campaign resulted in the discovery of **19a**. This very potent and selective compound efficiently reduced blood lymphocyte counts in rats, had an acceptable liability profile, and had desirable pharmacokinetic and pharmacodynamic properties. Furthermore, studies in two preclinical models of arthritis and multiple sclerosis demonstrated **19a** to have robust efficacy. In comparison to our first development candidate (**4**), compound **19a** exhibited similar in vitro activity and comparable efficacy in two pre-clinical disease models (Rat AA and mouse EAE); however, the PK/PD profile of **19a** was more consistent across multiple species (mouse, rat, monkey and dog). On the basis of these encouraging results, **19a** was progressed to advanced studies for consideration as a clinical development candidate.

Experimental Section:

Biological Assays

$S1P_1$ Binding Assay:

Membranes were prepared from CHO cells expressing human $S1P_1$. Cells were dissociated in buffer containing 20 mM HEPES, pH 7.5, 50 mM NaCl, 2 mM EDTA and Protease Inhibitor cocktail (Roche), and disrupted on ice using the Polytron homogenizer. The homogenate was centrifuged at 20,000 rpm (48,000G) and the supernatant was discarded. The membrane pellets were resuspended in buffer containing 50 mM HEPES, pH 7.5, 100 mM NaCl, 1 mM $MgCl_2$, 2 mM EDTA and stored in aliquots at -80°C after protein concentration determination. Membranes (2 μg/well) and 0.03 nM final concentration of ^{33}P-S1P ligand (1 mCi/ml, American Radiolabeled Chemicals) were added to the compound plates. Binding was performed for 45

minutes at room temperature, terminated by collecting the membranes onto GF/B filter plates, and radioactivity was measured by TopCount. The competition data of the test compounds over a range of concentrations was plotted as percentage inhibition of radioligand specific binding. The IC_{50} is defined as the concentration of competing ligand needed to reduce specific binding by 50%.

Receptor [^{35}S] GTPγS Binding Assays

Compounds were loaded in a 384 Falcon v-bottom plate (0.5 μl/well in a 3-fold dilution). Membranes prepared from $S1P_1$/CHO cells or EDG3-Ga15-bla HEK293T cells were added to the compound plate (40 μl/well, final protein 3 μg/well) with multidrop. [^{35}S]GTP (1250 Ci/mmol, Perkin Elmer) was diluted in assay buffer: 20 mM HEPES, pH7.5, 10 mM $MgCl_2$, 150 mM NaCl, 1 mM EGTA, 1 mM DTT, 10 μM GDP, 0.1% fatty acid free BSA, and 10 μg/ml Saponin to 0.4 nM. 40 μl of the [^{35}S] GTP solution was added to the compound plate with a final concentration of 0.2 nM. The reaction was kept at room temperature for 45 min. At the end of incubation, all the mixtures in the compound plate were transferred to a 384 well FB filter plates via GPCR robot system. The filter plate was washed with water 4 times by using the modified manifold Embla plate washer and dried at 60°C for 45 min. 30 μl of MicroScint 20 scintillation fluid was added to each well for counting at Packard TopCount. EC_{50} is defined as the agonist concentration that corresponds to 50% of the Ymax (maximal response) obtained for each individual compound tested.

Blood Lymphocyte Reduction Assay (BLR) in Rodents:

Lewis rats were dosed orally with test article (as a solution or suspension in the vehicle) or vehicle alone (polyethylene glycol 300, "PEG300"). Blood was drawn at 4 hr and at 24 hr by

retro-orbital bleeding. Blood lymphocyte counts were determined on an ADVIA 120 Hematology Analyzer (Siemens Healthcare Diagnostics). The results were measured as a reduction in the percentage of circulating lymphocytes as compared to the vehicle treated group at the 4 hr and 24 hr measurements. The results represent the average results of all animals within each treatment group (n = 3-4).

Rat Adjuvant Induced Arthritis Assay (AA)

Male Lewis rats (150-175 g; Harlan, n=8 treatment group) were immunized at the base of the tail with 100 μl of 10 mg/ml freshly ground Mycobacterium butyricum (Difco Laboratories) in incomplete Freund's adjuvant (sigma). Animals were dosed once daily with the test article (as a solution or suspension in the vehicle) or vehicle alone (polyethylene glycol 300, "PEG300") starting from the day of immunization. The volumes of their hind paws were measured in a water displacement plethysmometer (Ugo Basile, Italy). The baseline paw measurements were taken before onset of the disease (between day 7 to day 10). The paw measurements were then taken three times a week until the end of the study on day 20. All procedures involving animals were reviewed and approved by the Institutional Animal Care Use Committee.

Mouse Experimental Autoimmune Encephalomyelitis Assay (EAE)

Mice (C57BL/6 female, 6-8 weeks of age, Charles River, n=10-12 treatment group) were immunized subcutaneously with 150 μg MOG35-55 emulsified 1:1 with incomplete Freund's adjuvant (sigma) supplemented with 150 μg Mycobacterium tuberculosis H37RA (Difco Laboratories). 400 ng of pertussis toxin (CalBiochem) was injected intraperitoneally on the day of immunization and two days later. Animals were dosed once daily with the test article (as a solution or suspension in the vehicle) or vehicle alone (polyethylene glycol 300, "PEG300")

starting from 1 day after immunization. Clinical scoring and body weight were taken 3 times per week until the end of the study on day 24. Clinical scoring system: 0.5: partial tail weakness; 1: limp tail or waddling gait with tail tonicity; 1.5: waddling gait with partial tail weakness; 2: waddling gait with limp tail (ataxia); 2.5: ataxia with partial limb paralysis; 3: full paralysis of one limb; 3.5: full paralysis of one limbs with partial paralysis of a second limb; 4: full paralysis of two limbs; 4.5: moribund; 5: death.

$S1P_1$ Internalization Assay.

$hS1P_1$ internalization assay: For quantification of S1P-1 expression using a high content system, GFP was fused to $hS1P_1$ at its C-terminus and a stable CHO cell line expressing $hS1P_1$/GFP was established. Cells were suspended in assay medium (F12 medium with 5 % Charcoal-Dextran treated FBS, 20mM HEPES, and 1X Pen/Strep) at 7.5x104 cells/ml and plated into 384 well plates (in 20 μl, 1,500 cells/well final) with a Multidrop liquid handler (Thermo Scientific, Waltham, MA). Cell plates were incubated at 37 ºC for 48 hr. Titrated S1P and BMS compounds were dispensed into the cell plates (concentration range from 100 μM to 0.005 μM) and the plates were further incubated at 37 ºC for 50 min. Cells were fixed by adding 10 μl of fixation buffer (7.4% v/v formaldehyde containing 15 μM Draq5 in DPBS) directly onto the assay medium and incubated for 15 min at rt followed by two washes with DPBS. This was followed by the addition of 50 μl DPBS to the cell layer and the plates were sealed with a transparent plate seal (Perkin Elmer #6005185). Imaging was carried out using the Evotec Opera High Content Confocal System (Perkin Elmer, Boston, MA) equipped with 3 diode lasers, peltier cooled CCD camera detector and a Nipkow spinning disk. Cell images were quantified using a membrane fluorescent scoring algorithm. Data was analyzed using a customized HTS data analysis software package. EC_{50} values were determined using XL-Fit software program.

Molecular Modelling Methods.

All modeling calculations were carried out using Maestro v2015-1 (Schrodinger LLC). The S1P1 crystal structure in complex with **24** (RCSB ID 3V2W) was the receptor template used for docking studies. The protein was prepared using the Protein Prep module following the default protocols. Candidate compounds were docked with Glide into a binding site centered on the crystallographic ligand and including residues within 5A of the ligand. Compounds were docked without constraints and 20 poses returned. Favorable poses were selected by visual inspection and minimized using the Protein Refinement Minimize module. The ligand and residues within 5A were freely mobile, with the remainder frozen. The final pose was selected from the minimized complexes via visual inspection.

Chemistry. All commercially available chemicals and solvents were used without further purification. Reactions were performed under an atmosphere of nitrogen. All flash column chromatography was performed on EM Science silica gel 60 (particle size of 40 – 60 μm). All new compounds gave satisfactory ^{1}H NMR, LC/MS and/or HRMS, and mass spectrometry results. ^{1}H NMR spectra were obtained on a Bruker 400 MHz or a JEOL 500 MHz NMR spectrometer using the residual signal of deuterated NMR solvent as internal reference. Electrospray ionization (ESI) mass spectra were obtained on a Waters ZQ single quadrupole mass spectrometer. High-resolution mass spectral analysis was performed on an LTQ-FT mass spectrometer interfaced to a Waters Acquity ultraperformance liquid chromatography.

HPLC analyses were performed using the following conditions. All final compounds had an HPLC purity of ≥95%.

Method A: A linear gradient using 10% methanol, 90% water, and 0.1% TFA (Solvent A) and 90% methanol, 10% water, and 0.1% TFA (Solvent B); *t* = 0 min., 0% B, *t* = 2 min., 100% B (1 min.) was employed on a Waters Sunfire C18 5 μm 4.6x 30mm column. Flow rate was 5.0 ml/min and UV detection was set to 220/254 nm. The LC column was maintained at ambient temperature.

Method B: A linear gradient using 10% methanol, 90% water, and 0.1% TFA (Solvent A) and 90% methanol, 10% water, and 0.1% TFA (Solvent B); *t* = 0 min., 0% B, *t* = 4 min., 100% B (1 min. hold) was employed on a Waters Sunfire C18 4.6 x 50 mm column. Flow rate was 4.0 ml/min and UV detection was set to 220/254 nm. The LC column was maintained at ambient temperature.

Method C. A linear gradient using 5% CH_3CN, 95% water with 10 μM ammonium acetate (Solvent A) and 95% CH_3CN, 5% water with 10 mM ammonium acetate (Solvent B); *t* = 0 min., 0% B, *t* = 4 min., 100% B (1 min. hold) was employed on a Supelco Ascentis Express C18, 4.6 x 50 mm, 2.7-μm particles column. Flow: 4 mL/min. The LC column was maintained at ambient temperature.

Method E: A linear gradient using 10% methanol, 90% water, and 0.1% TFA (Solvent A) and 90% methanol, 10% water, and 0.1% TFA (Solvent B); *t* = 0 min., 0% B, *t* = 4 min., 100% B (1 min. hold) was employed on a Chromolith SpeedROD 4.6 x 50 mm column. Flow rate was 4.0 ml/min. The LC column was maintained at ambient temperature.

Method F: A linear gradient using 5% acetonitrile, 95% water, and 0.05% TFA (Solvent A) and 95% acetonitrile, 5% water, and 0.05% TFA (Solvent B); *t* = 0 min., 10% B, *t* = 15 min., 100% B (20 min.) was employed on a SunFire C18 3.5 μm 4.6 x 150 mm column. Flow rate was 1.0

ml/min and UV detection was set to 220/254 nm. The LC column was maintained at ambient temperature.

Method G: A linear gradient using 5% acetonitrile, 95% water, and 0.05% TFA (Solvent A) and 95% acetonitrile, 5% water, and 0.05% TFA (Solvent B); *t* = 0 min., 10% B, *t* = 15 min., 100% B (20 min.) was employed on a XBridge Ph 3.5 μm 4.6 x 150 mm column. Flow rate was 1.0 ml/min and UV detection was set to 220/254 nm. The LC column was maintained at ambient temperature.

Method H: A linear gradient using 5:95 acetonitrile:water with 10 mM ammonium acetate and 95:5 acetonitrile:water with 10 mM ammonium acetate; *t* = 0 min., 0% B, *t* = 4 min., 100% B, then a 1-minute hold at 100% B was employed on a Supelco Ascentis Express C18 column (4.6 x 50 mm, 2.7-μm particles). Flow rate was 4 mL/min. Temperature 45 °C.

Method I: A linear gradient using 5:95 acetonitrile:water with 0.05% TFA and 95:5 acetonitrile:water with 0.05% TFA; *t* = 0 min., 0% B, *t* = 4 min., 100% B, then a 1-minute hold at 100% B was employed on a Supelco Ascentis Express C18 column (4.6 x 50 mm, 2.7-μm particles). Flow rate was 4 mL/min. Temperature 45 °C.

5-phenyl-4-propylisoxazole-3-carboxylic acid (5).[27]

Pent-1-ynylbenzene (17 mL, 106 mmol) and diethyl 2-nitromalonate (30 mL, 172 mmol) were placed in a stainless steel pressure bomb and heated to 160°C for 18 hours. The reaction mixture was cooled in an ice bath then the remaining pressure was slowly released. The reaction mixture was diluted with EtOAc and washed with 1N NaOH. The aqueous layer was back extracted once. The organic layer was dried over $MgSO_4$, filtered, and concentrated. The crude material was treated with 1N NaOH/EtOH at 75°C for two hours. Diluted with water and

washed with EtOAc. The aqueous layer was separated, acidified with concentrated HCl, and extracted with EtOAc. The organic layer was dried with $MgSO_4$, filtered and concentrated to afford 20 g of 5-phenyl-4-propylisoxazole-3-carboxylic acid as a white solid (**5,** 86%). ^{1}H NMR (400 MHz, *DMSO-d*$_6$) δ ppm 7.61 - 7.67 (2 H, m), 7.43 - 7.57 (3 H, m), 2.65 - 2.73 (2 H, m), 1.47 - 1.58 (2 H, m), 0.85 (3 H, t, *J*=7.36 Hz). MS $(M+H)^+$ at *m/z* 232; HPLC t_r = 3.37 minutes (Method A).

N'-hydroxy-4-vinylbenzimidamide (**6**).[27]

To a solution of 4-vinylbenzonitrile (4.4 g, 34 mmol) and hydroxylamine hydrochloride (4.7 g, 67.5 mmol) in 2-propanol (50 mL) was added sodium bicarbonate (11.3 g, 135 mmol). The reaction was heated at 80°C for 2 hours. The reaction mixture was diluted with EtOAc and washed with water. The organic layer was dried with $MgSO_4$, filtered, and concentrated to afford 5.3 g of N'-hydroxy-4-vinylbenzimidamide (**6,** 96%). ^{1}H NMR (500 MHz, *DMSO-d*$_6$) δ ppm 9.65 (1 H, s), 7.64 (2 H, d, *J*=8.52 Hz), 7.46 (2 H, d, *J*=8.25 Hz), 6.73 (1 H, dd, *J*=17.73, 10.86 Hz), 5.86 (1 H, d, *J*=17.87 Hz), 5.80 (2 H, s), 5.27 (1 H, d, *J*=11.82 Hz). MS $(M+H)^+$ at *m/z* 163; HPLC t_r = 0.57 minutes (Method A).

5-(5-phenyl-4-propylisoxazol-3-yl)-3-(4-vinylphenyl)-1,2,4-oxadiazole (7).[27]

To a mixture of 5-phenyl-4-propylisoxazole-3-carboxylic acid (**5**), (3 g, 13 mmol) and pyridine (1 mL, 13 mmol) in DCM (50 mL) was added cyanuric fluoride (1.1 mL, 13 mmol). The reaction mixture was stirred 1 hour at room temperature. The reaction mixture was diluted with DCM (50 mL) and washed with 1M HCl. The organic layer was dried over $MgSO_4$, filtered, and concentrated. The residue was dissolved in CH_3CN (50 mL) then **6** (2.1 g, 13 mmol) and DIEA (3.40 mL, 19.5 mmol) were added. The mixture was heated at 70°C overnight. The

reaction mixture was diluted with EtOAc and washed with saturated KH_2PO_4. The organic layer was dried with $MgSO_4$, filtered, and concentrated to afford 4.6 g of 5-(5-phenyl-4-propylisoxazol-3-yl)-3-(4-vinylphenyl)-1,2,4-oxadiazole as a solid (**7,** 45%). ^{1}H NMR (400MHz, $CDCl_3$) d 8.19 (d, J=8.4 Hz, 2H), 7.80 (dd, J=8.0, 1.7 Hz, 2H), 7.64 - 7.52 (m, 5H), 6.82 (dd, J=17.6, 10.8 Hz, 1H), 5.91 (dd, J=17.6, 0.4 Hz, 1H), 5.42 (d, J=11.4 Hz, 1H), 3.15 - 2.97 (m, 2H), 1.96 - 1.70 (m, 2H), 1.09 (t, J=7.4 Hz, 3H); MS $(M+H)^+$ at *m/z* 358; HPLC t_r = 2.34 minutes (Method A).

3-(4-(oxiran-2-yl)phenyl)-5-(5-phenyl-4-propylisoxazol-3-yl)-1,2,4-oxadiazole (8).[27]

To a mixture of 5-(5-phenyl-4-propylisoxazol-3-yl)-3-(4-vinylphenyl)-1,2,4-oxadiazole (4.6 g, 13 mmol) in DCM (500 mL) was added m-CPBA (9 g, 52 mmol). The reaction mixture was stirred overnight at room temperature. Next, the reaction mixture was washed with 1N NaOH. The organic layer was dried with $MgSO_4$, filtered, and concentrated to afford 3g of 3-(4-(oxiran-2-yl)phenyl)-5-(5-phenyl-4-propylisoxazol-3-yl)-1,2,4-oxadiazole as a solid (**8,** 62%). ^{1}H NMR (400 MHz, *CDCl$_3$*) δ ppm 8.16 - 8.22 (2 H, m), 7.78 (2 H, dd, *J*=8.02, 1.65 Hz), 7.50 - 7.59 (3 H, m), 7.46 (2 H, d, *J*=8.13 Hz), 3.95 (1 H, dd, *J*=4.06, 2.53 Hz), 3.22 (1 H, dd, *J*=5.49, 4.17 Hz), 2.98 - 3.06 (2 H, m), 2.85 (1 H, dd, *J*=5.49, 2.64 Hz), 1.72 - 1.83 (2 H, m), 1.06 (3 H, t, *J*=7.25 Hz). MS $(M+H)^+$ at *m/z* 374; HPLC t_r = 4.31 minutes (Method B).

2-(2-hydroxy-2-(4-(5-(5-phenyl-4-propylisoxazol-3-yl)-1,2,4-oxadiazol-3-yl)phenyl)ethyl)isoindoline-1,3-dione.[27]

To a mixture of 3-(4-(oxiran-2-yl)phenyl)-5-(5-phenyl-4-propylisoxazol-3-yl)-1,2,4-oxadiazole (100 mg, 0.27 mmol) and phthalimide (43 mg, 0.30 mmol) in DMF (2 mL) was added potassium phthalimide, (6 mg, 0.032 mmol). Heated to 100 °C overnight. The reaction mixture was diluted with EtOAc and washed with sat. NaCl. The organic layer was dried with

$MgSO_4$, filtered and concentrated. Purified by HPLC. HPLC conditions: Phenomenex Luna C18 5 μm column (250 x 30mm); 50-100% CH_3CN/water (0.1% TFA); 25 minute gradient; 30 mL/min. Recovered 85 mg of 2-(2-hydroxy2-(4-(5-(5-phenyl-4-propylisoxazol-3-yl)-1,2,4-oxadiazol-3-yl)phenyl)ethyl)isoindoline-1,3-dione (61%). ^{1}H NMR (400 MHz, *CDCl$_3$*) δ ppm 8.15 - 8.24 (2 H, m), 7.86 (2 H, dd, *J*=5.49, 3.08 Hz), 7.75 - 7.79 (2 H, m), 7.74 (2 H, dd, *J*=5.27, 3.08 Hz), 7.61 - 7.66 (2 H, m), 7.50 - 7.59 (4 H, m), 5.18 (1 H, dd, *J*=8.02, 3.63 Hz), 3.96 - 4.12 (2 H, m), 2.98 - 3.05 (2 H, m), 1.71 - 1.82 (2 H, m), 1.06 (3 H, t, *J*=7.36 Hz). MS $(M+H)^+$ at *m/z* 521; HPLC t_r = 4.22 minutes (Method B).

2-amino-1-(4-(5-(5-phenyl-4-propylisoxazol-3-yl)-1,2,4-oxadiazol-3-yl)phenyl)ethanol (9).[27]

To a mixture of 2-(2-hydroxy-2-(4-(5-(5-phenyl-4-propylisoxazol-3-yl)-1,2,4-oxadiazol-3-yl)phenyl)ethyl)isoindoline-1,3-dione (75 mg, 0.14 mmol) in ethanol (5 mL) was added hydrazine monohydrate (1 mL, 20.6 mmol). Heated at 80 °C for two hours. The reaction mixture was diluted with EtOAc and washed with sat NaCl. The organic layer was dried with $MgSO_4$, filtered and concentrated. The material was dissolved in CH_3CN and purified by HPLC. HPLC conditions: Phenomenex Luna C18 5 μm column (250 x 30mm); 25-100% CH_3CN/water (0.1% TFA); 25 minute gradient; 30 mL/min. Recovered 30 mg of 2-amino-1-(4-(5-(5-phenyl-4-propylisoxazol-3-yl)-1,2,4-oxadiazol-3-yl)phenyl)ethanol as a white solid (**9**, 55%). ^{1}H NMR (400 MHz, *DMSO-d$_6$*) δ ppm 8.08 (2 H, d, *J*=8.35 Hz), 7.88 (2 H, br. s.), 7.74 - 7.80 (2 H, m), 7.53 - 7.64 (5 H, m), 6.22 (1 H, d, *J*=3.95 Hz), 4.82 - 4.88 (1 H, m), 3.07 (1 H, dd, *J*=12.74, 2.86 Hz), 2.91 - 2.98 (2 H, m), 2.84 (1 H, dd, *J*=12.74, 9.67 Hz), 1.60 - 1.68 (2 H, m), 0.92 (3 H, t, *J*=7.36 Hz). MS $(M+H)^+$ at *m/z* 391; HPLC purity: 95.1%; t_r = 7.51 min. (Method E); 96.1%; t_r = 8.06 min. (Method F).

2-bromo-1-(4-(5-(5-phenyl-4-propylisoxazol-3-yl)-1,2,4-oxadiazol-3-yl)phenyl)ethanol(10).[27]

To a mixture of 3-(4-(oxiran-2-yl)phenyl)-5-(5-phenyl-4-propylisoxazol-3-yl)-1,2,4-oxadiazole (205 mg, 0.55 mmol) in THF (5 mL) at -78°C was slowly added bromotriethylsilane (100 µL, 0.58 mmol). The reaction mixture was stirred for 1 hour at -78°C. The reaction was quenched with water and extracted with EtOAc. The organic layer was dried with $MgSO_4$, filtered, and concentrated. The solids were purified on a silica cartridge using an EtOAc/hexanes gradient to afford 130 mg of 2-bromo-1-(4-(5-(5-phenyl-4-propylisoxazol-3-yl)-1,2,4-oxadiazol-3-yl)phenyl)ethanol (**10,** 52%) as a white solid. ^{1}H NMR (400 MHz, *CDCl$_3$*) δ ppm 8.16-8.24 (2 H, m), 7.72-7.81 (2 H, m), 7.61 (2 H, m, *J*=8.13 Hz), 7.49-7.58 (3 H, m), 5.12 (1 H, dd, *J*=7.47, 5.93 Hz), 4.09-4.17 (1 H, m), 4.01-4.08 (1 H, m), 2.97-3.05 (2 H, m), 1.70-1.83 (2 H, m), 1.06 (3 H, t, *J*=7.36 Hz). MS $(M+H)^+$ at *m/z* 455; HPLC t_r = 2.12 minutes (Method A).

3-((2-hydroxy-2-(4-(5-(5-phenyl-4-propylisoxazol-3-yl)-1,2,4-oxadiazol-3-yl)phenyl)ethyl)amino)propanoic acid (11a).[27]

To a mixture of **9** (27 mg, 0.069 mmol) in pyridine (1 mL) was added tert-butyl 3-bromopropanoate (0.012 mL, 0.069 mmol). Heated at 80 °C for one hour. The reaction mixture was cooled, filtered and purified by HPLC. HPLC conditions: Phenomenex Luna C18 5 µm column (250 x 30mm); 25-100% CH_3CN/water (0.1% TFA); 25 minute gradient; 30 mL/min. Isolated fractions with correct mass and freeze-dried overnight. Residue was treated with TFA/DCM (1:1) for 1 hour. Removed solvents in vacuo and freeze dried from CH_3CN. Recovered 3 mg of 3-((2-hydroxy-2-(4-(5-(5-phenyl-4-propylisoxazol-3-yl)-1,2,4-oxadiazol-3-yl)phenyl)ethyl)amino)propanoic acid, TFA salt as a white solid (**11a**, 9.4%). ^{1}H NMR (400 MHz, *DMSO-d$_6$*) δ ppm 8.64 (1 H, br. s.), 8.14 (2 H, d, *J*=8.35 Hz), 7.82 (2 H, dd, *J*=7.91, 1.76 Hz), 7.58 - 7.70 (5 H, m), 6.41 (1 H, br. s.), 5.01 (1 H, dd, *J*=10.00, 1.65 Hz), 3.18 - 3.30 (4 H, m), 2.94 - 3.03 (2 H, m), 2.71 (2 H, td, *J*=7.25, 2.20 Hz), 1.64 - 1.74 (2 H, m, *J*=7.56, 7.56, 7.56,

7.42, 7.25 Hz), 0.97 (3 H, t, *J*=7.25 Hz). MS $(M+H)^+$ at *m/z* 463; HPLC t_r = 3.4 minutes (Method B); HPLC purity: 99.4%; t_r = 8.73 min. (Method E); 99.8%; t_r = 7.51 min. (Method F).

1-(2-hydroxy-2-(4-(5-(5-phenyl-4-propylisoxazol-3-yl)-1,2,4-oxadiazol-3-yl)phenyl)ethyl)pyrrolidine-3-carboxylic acid (11b). [27]

To a mixture of **10** (30 mg, 0.066 mmol) and pyrrolidine-3-carboxylic acid (22.81 mg, 0.198 mmol) in DMSO (2 mL) was added DBU (0.030 mL, 0.198 mmol). The reaction mixture was heated at 80°C for 2 hours. The reaction mixture was filtered and purified by HPLC. HPLC conditions: Phenomenex Luna C18 5 μm column (250 x 30mm); 30-100% CH_3CN/water (0.1% TFA); 25 minute gradient; 30 mL/min. Recovered 16 mg of 1-(2-hydroxy-2-(4-(5-(5-phenyl-4-propylisoxazol-3-yl)-1,2,4-oxadiazol-3-yl)phenyl)ethyl)pyrrolidine-3-carboxylic acid, TFA salt **(11b**, 39%**)** as a clear oil. ^{1}H NMR (400 MHz, *MeOH-d*$_3$) δ ppm 8.21 (2 H, d, *J*=8.35 Hz), 7.81 (2 H, dd, *J*=8.02, 1.65 Hz), 7.69 (2 H, d, *J*=8.35 Hz), 7.54-7.66 (3 H, m), 5.10-5.22 (1 H, m), 3.39-3.54 (4 H, m), 3.24-3.27 (3 H, m), 3.00-3.10 (2 H, m), 2.23-2.57 (2 H, m), 1.70-1.83 (2 H, m), 1.05 (3 H, t, *J*=7.36 Hz). MS $(M+H)^+$ at *m/z* 489; HPLC t_r = 2.08 minutes (Method H). HPLC purity: 96%; t_r = 2.19 minutes (Method I).

The following compounds were synthesized using the same method as **11b**:

2-((*2S*)-1-(2-hydroxy-2-(4-(5-(5-phenyl-4-propylisoxazol-3-yl)-1,2,4-oxadiazol-3-yl)phenyl)ethyl)pyrrolidin-2-yl)acetic acid (11c).[27]

Recovered 9 mg of 2-((*2S*)-1-(2-hydroxy-2-(4-(5-(5-phenyl-4-propylisoxazol-3-yl)-1,2,4-oxadiazol-3-yl)phenyl)ethyl)pyrrolidin-2-yl)acetic acid, TFA salt **(11e**, 20%**)** as a pale yellow oil. ^{1}H NMR (400 MHz, *MeOH-d*$_3$) δ ppm 8.18 (4 H, d, *J*=8.35 Hz), 7.77-7.84 (2 H, m), 7.54-7.67 (5 H, m), 5.92-6.01 (1 H, m), 5.00-5.09 (2 H, m), 4.26-4.42 (1 H, m), 3.76-3.94 (1 H, m),

3.00-3.11 (2 H, m), 2.75-2.98 (2 H, m), 2.18-2.34 (1 H, m), 1.90-2.14 (2 H, m), 1.60-1.85 (3 H, m), 1.04 (3 H, t, *J*=7.25 Hz). MS $(M+H)^+$ at *m/z* 503; HPLC t_r = 3.50 minutes (Method B). HPLC purity: 98.6%; t_r = 9.08 min. (Method E).

2-(1-(2-hydroxy-2-(4-(5-(5-phenyl-4-propylisoxazol-3-yl)-1,2,4-oxadiazol-3-yl)phenyl)ethyl)piperidin-2-yl)acetic acid (11d).[27]

Recovered 9 mg of 2-(1-(2-hydroxy-2-(4-(5-(5-phenyl-4-propylisoxazol-3-yl)-1,2,4-oxadiazol-3-yl)phenyl)ethyl)piperidin-2-yl)acetic acid, TFA salt **(11d**, 20%**)** as a clear oil. ^{1}H NMR (400 MHz, MeOH-d3) δ ppm 8.14-8.25 (2 H, m), 7.80 (3 H, dd, *J*=8.02, 1.65 Hz), 7.66-7.74 (1 H, m), 7.53-7.66 (4 H, m), 5.04 (1 H, t, *J*=5.82 Hz), 5.00-5.35 (1 H, m), 4.35 (2 H, d, *J*=5.49 Hz), 3.80-4.02 (1 H, m), 3.70 (1 H, br. s.), 3.33-3.54 (4 H, m), 2.99-3.10 (2 H, m), 2.68-2.96 (1 H, m), 1.82-2.09 (2 H, m), 1.70-1.81 (2 H, m, *J*=15.27, 7.58, 7.47, 7.47 Hz), 1.40-1.70 (1 H, m), 1.04 (2 H, t, *J*=7.36 Hz). MS $(M+H)^+$ at *m/z* 517. HPLC t_r = 3.35 and 3.53 minutes in a 6 to 4 ratio of diastereomers (with respect to above LC retention times) (Method B). HPLC purity: 95.1%; t_r = 9.25-9.30 min. (Method E).

(*3S*)-1-(2-hydroxy-2-(4-(5-(5-phenyl-4-propylisoxazol-3-yl)-1,2,4-oxadiazol-3-yl)phenyl)ethyl)piperidine-3-carboxylic acid (11e).[27]

Recovered 60 mg of (*3S*)-1-(2-hydroxy-2-(4-(5-(5-phenyl-4-propylisoxazol-3-yl)-1,2,4-oxadiazol-3-yl)phenyl)ethyl)piperidine-3-carboxylic acid, TFA salt **(11e** 71%**)** as a white solid. ^{1}H NMR (400 MHz, *DMSO-d*$_6$) δ ppm 8.12 (2 H, dd, *J*=8.24, 1.87 Hz), 7.79 (2 H, dd, *J*=8.02, 1.65 Hz), 7.67 (2 H, d, *J*=8.35 Hz), 7.56-7.64 (3 H, m), 5.13-5.28 (1 H, m), 3.81 (1 H, d, *J*=11.86 Hz), 3.67 (2 H, t, *J*=14.17 Hz), 3.21-3.33 (3 H, m), 2.92-3.01 (2 H, m), 1.77-2.14 (2 H, m), 1.61-1.73 (2 H, m), 1.33-1.51 (1 H, m), 0.94 (1 H, s), 0.94 (3 H, t, *J*=7.36 Hz). MS $(M+H)^+$ at *m/z*

503; HPLC t_r = 3.37 minutes (Method B). HPLC purity: 97.3%; t_r = 9.10 min. (Method E); 97.4%; t_r = 7.75 min. (Method F).

(*3R*)-1-(2-hydroxy-2-(4-(5-(5-phenyl-4-propylisoxazol-3-yl)-1,2,4-oxadiazol-3-yl)phenyl)ethyl)piperidine-3-carboxylic acid (11f).[27]

Recovered 6 mg of (*3R*)-1-(2-hydroxy-2-(4-(5-(5-phenyl-4-propylisoxazol-3-yl)-1,2,4-oxadiazol-3-yl)phenyl)ethyl)piperidine-3-carboxylic acid, TFA salt (**11f**, 14%) as a white solid. ^{1}H NMR (400 MHz, *MeOH-d*$_3$) δ ppm 8.21 (2 H, d, *J*=7.91 Hz), 7.71 (2 H, dd, *J*=8.02, 1.65 Hz), 7.47-7.56 (5 H, m), 4.46 (1 H, br. s.), 4.10 (2 H, d, *J*=6.37 Hz), 3.25-3.61 (2 H, m), 2.92-3.03 (3 H, m), 2.91 (2 H, br. s.), 2.01-2.27 (1 H, m), 1.81-2.00 (3 H, m), 1.60-1.76 (2 H, m, *J*=7.61, 7.61, 7.61, 7.61, 7.36 Hz), 1.20-1.59 (1 H, m), 0.95 (3 H, t, *J*=7.36 Hz). MS $(M+H)^+$ at *m/z* 503; HPLC t_r = 3.32 minutes (Method B). HPLC purity: 95.9%; t_r = 7.55 min. (Method F).

(*1R,2S*)-2-(2-hydroxy-2-(4-(5-(5-phenyl-4-propylisoxazol-3-yl)-1,2,4-oxadiazol-3-yl)phenyl)ethylamino)cyclopentanecarboxylic acid (11g).[27]

Recovered 9 mg of (*1R,2S*)-2-(2-hydroxy-2-(4-(5-(5-phenyl-4-propylisoxazol-3-yl)-1,2,4-oxadiazol-3-yl)phenyl)ethylamino)cyclopentanecarboxylic acid, TFA salt **(11g**, 22%**)** as a clear oil. ^{1}H NMR (400 MHz, *MeOH-d*$_3$) δ ppm 8.20 (2 H, m, *J*=8.13 Hz), 7.76 - 7.83 (2 H, m), 7.67 (2 H, m, *J*=8.35 Hz), 7.52 - 7.64 (3 H, m), 5.10 (1 H, ddd, *J*=10.16, 3.68, 3.52 Hz), 3.70 - 3.81 (1 H, m), 3.15 - 3.27 (2 H, m), 2.99 - 3.08 (2 H, m), 2.17 - 2.29 (2 H, m), 2.05 - 2.16 (2 H, m), 1.86 - 1.99 (2 H, m), 1.70 - 1.82 (3 H, m), 1.04 (3 H, t, *J*=7.25 Hz). MS $(M+H)^+$ at *m/z*; HPLC t_r = 3.48 minutes (Method B); HPLC purity: 98.6%; t_r = 9.38 min. (Method E).

(*1S,2R*)-2-(2-hydroxy-2-(4-(5-(5-phenyl-4-propylisoxazol-3-yl)-1,2,4-oxadiazol-3-yl)phenyl)ethylamino)cyclopentanecarboxylic acid (11h).[27]

Recovered 7 mg of (*1S,2R*)-2-(2-hydroxy-2-(4-(5-(5-phenyl-4-propylisoxazol-3-yl)-1,2,4-oxadiazol-3-yl)phenyl)ethylamino)cyclopentanecarboxylic acid, TFA salt **(11h**, 17%**)** as a clear oil. ^{1}H NMR (400MHz, *MeOH-d*$_3$) δ 8.16 - 8.06 (m, 2H), 7.72 (dd, *J*=7.9, 1.5 Hz, 2H), 7.63 - 7.43 (m, 5H), 5.06 - 4.93 (m, 1H), 4.39 - 4.17 (m, 1H), 3.76 - 3.55 (m, 1H), 3.45 - 3.01 (m, 5H), 3.00 - 2.90 (m, 2H), 2.33 - 1.96 (m, 2H), 1.91 - 1.75 (m, 2H), 1.74 - 1.59 (m, 3H), 0.95 (t, *J*=7.4 Hz, 3H). MS $(M+H)^+$ at *m/z* 503; HPLC t_r = 3.48-3.56 minutes (Method B); HPLC purity: 98.4%; t_r = 9.35 min. (Method E); 96.1%; t_r = 8.1 min. (Method F).

1-(2-hydroxy-2-(4-(5-(5-phenyl-4-propylisoxazol-3-yl)-1,2,4-oxadiazol-3-yl)phenyl)ethyl)piperidin-3-ol (11i).[27]

To a mixture of piperidin-3-ol (20.04 mg, 0.198 mmol) in DMSO (2 mL) was added tetrabutylammonium hydroxide (0.198 mL, 0.198 mmol). After 5 minutes, **10** (30 mg, 0.066 mmol) was added. Heated at 80 °C for 2 hours. The reaction mixture was filtered and purified by HPLC. HPLC conditions: Phenomenex Luna C18 5 μm column (250 x 30mm); 25-100% CH_3CN/water (0.1% TFA); 25 minute gradient; 20 mL/min. Isolated fractions with correct mass and freeze-dried overnight. Recovered 22 mg of 1-(2-hydroxy-2-(4-(5-(5-phenyl-4-propylisoxazol-3-yl)-1,2,4-oxadiazol-3-yl)phenyl)ethyl)piperidin-3-ol, TFA salt **(11i**, 56%**)** as a clear oil. ^{1}H NMR (400MHz, DMSO-d6) δ 8.26 - 8.07 (m, 2H), 7.90 - 7.79 (m, 2H), 7.74 - 7.54 (m, 5H), 5.21 (d, J=9.2 Hz, 1H), 4.20 - 3.70 (m, 3H), 3.50 - 3.09 (m, 6H), 3.06 - 2.95 (m, 2H), 2.22 - 1.77 (m, 1H), 1.76 - 1.66 (m, 3H), 0.98 (t, J=7.4 Hz, 3H); MS $(M+H)^+$ at *m/z* 475. HPLC t_r = 3.32 minutes (Method B); HPLC Purity = 98.8; t_r = 8.89 min (Method E).

The following compounds were synthesized by the same method as **11i:**

4-(2-hydroxy-2-(4-(5-(5-phenyl-4-propylisoxazol-3-yl)-1,2,4-oxadiazol-3-yl)phenyl)ethyl)piperazine-2-carboxylic acid (11j).[27]

Recovered 5mg of 4-(2-hydroxy-2-(4-(5-(5-phenyl-4-propylisoxazol-3-yl)-1,2,4-oxadiazol-3-yl)phenyl)ethyl)piperazine-2-carboxylic acid, TFA salt **(11j**, 14%**)** as a clear oil. MS $(M+H)^+$ at *m/z* 504. HPLC Purity = 99%; t_r = 2.06 minutes (Method I).

2-(1-(2-hydroxy-2-(4-(5-(5-phenyl-4-propylisoxazol-3-yl)-1,2,4-oxadiazol-3-yl)phenyl)ethyl)piperidin-3-yl)acetic acid (11k).[27]

Recovered 6 mg of 2-(1-(2-hydroxy-2-(4-(5-(5-phenyl-4-propylisoxazol-3-yl)-1,2,4-oxadiazol-3-yl)phenyl)ethyl)piperidin-3-yl)acetic acid, TFA salt **(11k**, 16%**)** as a clear oil. MS $(M+H)^+$ at *m/z* 517. HPLC t_r = 2.08 min (Method C). Purity = 100%.

2-((*3R*)-1-(2-hydroxy-2-(4-(5-(5-phenyl-4-propylisoxazol-3-yl)-1,2,4-oxadiazol-3-yl)phenyl)ethyl)piperidin-3-yl)acetic acid (11l).[27]

Recovered 9 mg of 2-((*3R*)-1-(2-hydroxy-2-(4-(5-(5-phenyl-4-propylisoxazol-3-yl)-1,2,4-oxadiazol-3-yl)phenyl)ethyl)piperidin-3-yl)acetic acid, TFA salt **(11l**, 15%**)** as a white solid. ^{1}H NMR (400 MHz, *MeOH-d*$_3$) δ ppm 8.11 (2 H, m), 7.68-7.75 (2 H, m), 7.59 (2 H, m, *J*=8.35 Hz), 7.43-7.55 (3 H, m), 5.16 (1 H, dd, *J*=9.01, 4.61 Hz), 3.71-3.89 (1 H, m), 3.50-3.67 (2 H, m), 3.24 (1 H, d, *J*=2.42 Hz), 2.96 (2 H, dd, *J*=8.90, 6.92 Hz), 2.83-2.93 (1 H, m), 2.72 (1 H, td, *J*=11.86, 5.27 Hz), 2.16-2.39 (3 H, m), 1.77-2.00 (3 H, m), 1.59-1.75 (2 H, m, *J*=7.61, 7.61, 7.61, 7.61, 7.36 Hz), 1.13-1.32 (1 H, m), 0.95 (3 H, t, *J*=7.25 Hz). MS $(M+H)^+$ at *m/z* 517; HPLC t_r = 3.32

minutes (Method B). HPLC purity: 99.2%; t_r = 9.08 min. (Method E); 95.0%; t_r = 7.77 min. (Method F).

2-((*3S*)-1-(2-hydroxy-2-(4-(5-(5-phenyl-4-propylisoxazol-3-yl)-1,2,4-oxadiazol-3-yl)phenyl)ethyl)piperidin-3-yl)acetic acid (11m).[27]

Recovered 5 mg of 2-((*3S*)-1-(2-hydroxy-2-(4-(5-(5-phenyl-4-propylisoxazol-3-yl)-1,2,4-oxadiazol-3-yl)phenyl)ethyl)piperidin-3-yl)acetic acid, TFA salt **(11m**, 11%**)** as a white solid. ^{1}H NMR (400 MHz, *MeOH-d*$_3$) δ ppm 8.12 (2 H, m, *J*=8.35 Hz), 7.69-7.75 (2 H, m), 7.60 (2 H, m, *J*=8.13 Hz), 7.43-7.55 (3 H, m), 5.16 (1 H, dd, *J*=9.34, 4.50 Hz), 3.71-3.89 (1 H, m), 3.52-3.68 (3 H, m), 3.23-3.28 (1 H, m), 2.96 (2 H, dd, *J*=8.90, 6.92 Hz), 2.84-2.92 (1 H, m), 2.17-2.38 (3 H, m), 1.76-1.93 (3 H, m), 1.62-1.73 (2 H, m), 1.21 (1 H, dd, *J*=12.30, 4.17 Hz), 0.95 (3 H, t, *J*=7.25 Hz). MS $(M+H)^+$ at *m/z* 517; HPLC t_r = 3.37 minutes (Method B). HPLC purity: 97.6%; t_r = 9.1 min. (Method E).

tert-butyl 1-(2-(4-cyanophenyl)-2-oxoethyl)azetidine-3-carboxylate, hydrobromide[27]

To a mixture of 4-(2-bromoacetyl)benzonitrile (448 mg, 2 mmol) in toluene (10 mL) was added tert-butyl azetidine-3-carboxylate (346 mg, 2.2 mmol). Stirred overnight at rt. Removed solvent in vacuo and triturated residue with EtOAC. Solid was collected and dried in vacuo. Recovered 170 mg of tert-butyl 1-(2-(4-cyanophenyl)-2-oxoethyl)azetidine-3-carboxylate **(**28%**)** as a solid. MS $(M+H)^+$ at *m/z* 301; HPLC t_r = 0.93 minutes (Method A).

tert-butyl 1-(2-(4-cyanophenyl)-2-hydroxyethyl)azetidine-3-carboxylate (12)[27]

To a mixture of tert-butyl 1-(2-(4-cyanophenyl)-2-oxoethyl)azetidine-3-carboxylate (170 mg, 0.446 mmol) in ethanol (5 mL) was added sodium borohydride (25 mg, 0.661 mmol). Stirred for 1 hour. Quenched with water then diluted with ethyl acetate and washed with water.

The organic layer was dried with MgSO4, filtered and concentrated. Recovered 100 mg of tert-butyl 1-(2-(4-cyanophenyl)-2-hydroxyethyl)azetidine-3-carboxylate (74%) as a solid. MS $(M+H)^+$ at *m/z* 303; HPLC t_r = 0.91 minutes (Method A).

tert-butyl-1-(2-hydroxy-2-(4-(N'-hydroxycarbamimidoyl)phenyl)ethyl)azetidine-3-carboxylate[27]

To a mixture of **12** (100 mg, 0.331 mmol) and sodium bicarbonate (111 mg, 1.323 mmol) in 2-propanol was added hydroxylamine hydrochloride (22.98 mg, 0.331 mmol). Heated at 80 °C for 12 hours. The reaction mixture was diluted with ethyl acetate and washed with water. The organic layer was dried with MgSO4, filtered and concentrated. Recovered 110 mg of tert-butyl-1-(2-hydroxy-2-(4-(N'-hydroxycarbamimidoyl)phenyl)ethyl)azetidine-3-carboxylate. MS $(M+H)^+$ at *m/z* 336; HPLC t_r = 1.2 minutes (Method A).

3-Phenyl-4-(trifluoromethyl)isoxazole-5-carbonyl fluoride[21,27]

To a mixture of 3-phenyl-4-(trifluoromethyl)isoxazole-5-carboxylic acid[21,27] (3 g, 11.7 mmol) and pyridine (1.1 mL, 14.0 mmol) in dichloromethane (100 mL) at room temperature was added 2,4,6-trifluoro-1,3,5-triazine (cyanuric fluoride) (1.2 mL, 14.0 mmol). The reaction mixture was stirred at room temperature overnight, then diluted with dichloromethane (300 mL), washed with an ice-cold solution of 0.5N aqueous hydrochloric acid (2 x 100 mL), and the organic layer was collected. The aqueous layer was back-extracted with dichloromethane (200 mL), and the combined organic layers were dried with anhydrous sodium sulfate and concentrated to afford 2.9 g of 3-phenyl-4-(trifluoromethyl)isoxazole-5-carbonyl fluoride (91%) as a solid. The product was found to react readily with methanol and on analysis was

characterized as the methyl ester. HPLC t_r = 2.56 minutes (Method E); MS $(M+H)^+$ at *m/z* 272 (methyl ester).

1-(2-hydroxy-2-(4-(5-(3-phenyl-4-(trifluoromethyl)isoxazol-5-yl)-1,2,4-oxadiazol-3-yl)phenyl)ethyl)azetidine-3-carboxylic acid (13)[27]

To a mixture of 3-phenyl-4-(trifluoromethyl)isoxazole-5-carbonyl fluoride (86 mg, 0.33 mmol) and ((E)-tert-butyl 1-(2-hydroxy-2-(4-(N'-hydroxycarbamimidoyl)phenyl)ethyl)azetidine-3-carboxylate (111 mg, 0.33 mmol) in CH_3CN (10 mL) was added DIEA (0.115 mL, 0.660 mmol). After 1 hour, 1M TBAF in THF (0.330 mL, 0.330 mmol) was added and the reaction was stirred overnight. The reaction mixture was diluted with ethyl acetate and washed with water. The organic layer was dried with $MgSO_4$, filtered and concentrated. Crude residue was treated with TFA/DCM (1:1, 1 mL) to remove t-butyl ester. Concentrated in vacuo and purified by HPLC. Recovered 36 mg of 1-(2-hydroxy-2-(4-(5-(3-phenyl-4-(trifluoromethyl)isoxazol-5-yl)-1,2,4-oxadiazol-3-yl)phenyl)ethyl)azetidine-3-carboxylic acid, TFA salt (**13**, 17%) as a white solid. ^{1}H NMR (400MHz, *CD_3OD*) δ 8.22 (d, *J*=8.3 Hz, 2H), 7.68 (d, *J*=8.3 Hz, 5H), 7.63 - 7.52 (m, 3H), 5.04 (dd, *J*=10.1, 3.1 Hz, 1H), 3.73 (br. s., 1H), 3.61 - 3.38 (m, 2H), 3.26 - 3.16 (m, 4H);); MS $(M+H)^+$ at *m/z* 501; HPLC t_r = 3.23 minutes (Method B); HPLC purity: 96.5%; t_r = 5.19 min. (Method E);

(*S*)-ethyl 1-(2-(4-cyanophenyl)-2-oxoethyl)piperidine-3-carboxylate hydrobromide.[27]

To a solution of commercially available (*S*)-ethyl piperidine-3-carboxylate (10 g, 63.6 mmol) in 200 mL toluene was added 4-(2-bromoacetyl)benzonitrile (17g, 76 mmol). The reaction mixture was stirred overnight. The next day, the precipitated solid was collected by filtration and washed with EtOAc then dried under vacuum to afford 15.2 g of (*S*)-ethyl 1-(2-(4-

cyanophenyl)-2-oxoethyl)piperidine-3-carboxylate hydrobromide (63%) as a solid. ^{1}H NMR (400MHz, *CDCl$_3$*) δ 8.13 (d, *J*=8.3 Hz, 2H), 7.81 (d, *J*=8.3 Hz, 2H), 5.10 (q, *J*=18.3 Hz, 2H), 4.13 (q, *J*=7.0 Hz, 2H), 3.99 - 3.66 (m, 2H), 3.61 - 3.25 (m, 2H), 2.64 - 2.21 (m, 2H), 2.11 - 1.76 (m, 2H), 1.74 - 1.49 (m, 1H), 1.25 (t, *J*=7.3 Hz, 3H); MS $(M+H)^+$ at *m/z* 301; HPLC t_r = 1.51 minutes (Method B).

ethyl 1-((*S*)-2-(4-cyanophenyl)-2-hydroxyethyl)piperidine-3-carboxylate (14).[27]

To a mixture of (*S*)-ethyl 1-(2-(4-cyanophenyl)-2-oxoethyl)piperidine-3-carboxylate hydrobromide (1.3 g, 8.3 mmol) in ethanol (20 mL) was added sodium borohydride (315 mg, 8.27 mmol) portionwise. After 1 hour, the reaction mixture was quenched with water. The reaction mixture was diluted with EtOAc and washed with sat. NaCl. The organic layer was dried with $MgSO_4$, filtered, concentrated, and purified on a silica gel cartridge using a EtOAc/hexanes gradient to afford 2.0 g of (*S*)-ethyl 1-(-2-(4-cyanophenyl)-2-hydroxyethyl)piperidine-3-carboxylate as a mixture of diastereomers (**14**). ^{1}H NMR (400MHz, $CDCl_3$) δ 7.64 (d, J=8.4 Hz, 2H), 7.50 (d, J=7.9 Hz, 2H), 4.77 (dd, J=10.6, 3.5 Hz, 1H), 4.18 (q, J=7.0 Hz, 2H), 3.13 (d, J=9.0 Hz, 1H), 2.59 (dd, J=12.5, 3.5 Hz, 3H), 2.51 - 2.28 (m, 3H), 2.02 - 1.85 (m, 1H), 1.83 - 1.69 (m, 1H), 1.68 - 1.50 (m, 2H), 1.29 (t, J=7.2 Hz, 3H); HPLC t_r = 1.51 minutes (Method B).

(*S*)-ethyl 1-((*S*)-2-(4-cyanophenyl)-2-hydroxyethyl)piperidine-3-carboxylate (14a) and (*S*)-ethyl 1-((*R*)-2-(4-cyanophenyl)-2-hydroxyethyl)piperidine-3-carboxylate (14b).[27]

Compound **14** was separated by chiral HPLC (Berger SFC MGIII instrument equipped with a ChiralCel OJ (25 x 3 cm, 5 μm). Temp: 30°C; Flow rate: 130 mL/min; Mobile phase: CO_2/(MeOH + 0.1%DEA) in 9:1 ratio isocratic:

14a: Peak 1 (t_r = 2.9 min) from the chiral separation was isolated. The absolute and relative stereochemistry of compound **14a** was unambiguously assigned (*S,S*) by X-ray crystal structure.[22] ^{1}H NMR (400 MHz, *CDCl$_3$*) δ ppm 7.63 (2 H, m, *J*=8.35 Hz), 7.49 (2 H, m, *J*=8.35 Hz), 4.77 (1 H, dd, *J*=10.55, 3.52 Hz), 4.17 (2 H, q, *J*=7.03 Hz), 3.13 (1 H, d, *J*=9.23 Hz), 2.53-2.67 (3 H, m), 2.44 (2 H, dd, *J*=18.68, 9.89 Hz), 2.35 (1 H, dd, *J*=12.74, 10.55 Hz), 1.87-2.01 (1 H, m), 1.71-1.82 (1 H, m), 1.52-1.70 (2 H, m), 1.28 (3 H, t, *J*=7.03 Hz); MS $(M+H)^+$ at *m/z* 303; HPLC purity: 100% with > 99% d.e.; t_r = 2.56 min. (ChiralCel OJ (25 x 0.46 cm, 5 μm); Temp: 35°C; Flow rate: 2 mL/min; Mobile phase: CO_2/(MeOH + 0.1%DEA) in 8:2 ratio isocratic).

14b: Peak 2 (t_r = 3.8 min) from the chiral separation was isolated (>99% d.e.). The absolute and relative stereochemistry of **14b** was assigned (*S,R*) based on the crystal structure of **14a**. ^{1}H NMR (400 MHz, *CDCl$_3$*) δ ppm 7.63 (2 H, m, *J*=8.35 Hz), 7.49 (2 H, m, *J*=8.35 Hz), 4.79 (1 H, dd, *J*=10.55, 3.52 Hz), 4.16 (2 H, q, *J*=7.03 Hz), 2.69-2.91 (3 H, m), 2.60-2.68 (1 H, m), 2.56 (1 H, dd, *J*=12.30, 3.52 Hz), 2.36 (1 H, dd, *J*=12.52, 10.77 Hz), 2.25 (1 H, t, *J*=8.79 Hz), 1.65-1.90 (3 H, m), 1.52-1.64 (1 H, m, *J*=12.69, 8.49, 8.49, 4.17 Hz), 1.27 (3 H, t, *J*=7.25 Hz); MS $(M+H)^+$ at *m/z* 303; HPLC purity: 99.6% with > 99% d.e.; t_r = 2.95 min. (Method: ChiralCel OJ (25 x 0.46 cm, 5 μm). Temp: 35°C; Flow rate: 2 mL/min; Mobile phase: CO_2/(MeOH + 0.1%DEA) in 8:2 ratio isocratic).

(*R*)-ethyl 2-(1-(2-(4-cyanophenyl)-2-oxoethyl)piperidin-3-yl)acetate hydrobromide.[27]

To a mixture of 4-(2-bromoacetyl)benzonitrile (5.5 g, 24.5 mmol) in toluene was added (*R*)-ethyl 2-(piperidin-3-yl)acetate (4 g, 23.4 mmol). The reaction mixture was stirred for 4 days at room temperature and then stirred for one day at 50°C. Solvents were removed in vacuo. The resulting solids were triturated with EtOAc then collected and dried to afford 5 g of (*R*)-ethyl 2-

(1-(2-(4-cyanophenyl)-2-oxoethyl)piperidin-3-yl)acetate hydrobromide (70%) as a solid. ^{1}H NMR (400MHz, *DMSO-d$_6$*) δ 8.60 (br. s., 1H), 8.43 (br. s., 1H), 8.13 (s, 2H), 4.08 (q, *J*=7.1 Hz, 2H), 3.53 (br. s., 1H), 3.36 (br. s., 2H), 3.23 (d, *J*=11.9 Hz, 2H), 2.95 - 2.56 (m, 2H), 2.48 - 2.19 (m, 3H), 2.10 (ddt, *J*=14.9, 7.5, 3.7 Hz, 1H), 1.84 - 1.68 (m, 2H), 1.20 (t, *J*=7.2 Hz, 3H); MS $(M+H)^+$ at *m/z* 314; HPLC t_r = 0.77 minutes (Method A).

Ethyl 2-((3*R*)-1-(2-(4-cyanophenyl)-2-hydroxyethyl)piperidin-3-yl)acetate (15).[27]

To a mixture of (*R*)-ethyl 2-(1-(2-(4-cyanophenyl)-2-oxoethyl)piperidin-3-yl)acetate bydrobromide (1 g, 3.2 mmol) in ethanol (20 mL) was added sodium borohydride (0.120 g, 3.2 mmol). The reaction mixture was stirred for 1 hour. The reaction was quenched with water then diluted with EtOAc and washed with H_2O. The organic layer was dried with $MgSO_4$, filtered, and concentrated. The resulting solids were purified on a silica gel cartridge using an EtOAc/hexanes gradient to afford 575 mg of ethyl 2-((3*R*)-1-(2-(4-cyanophenyl)-2-hydroxyethyl)piperidin-3-yl)acetate as a mixture of diastereomers. ^{1}H NMR (400MHz, *CDCl$_3$*) δ 7.65 (d, *J*=8.4 Hz, 2H), 7.51 (d, *J*=8.1 Hz, 2H), 4.78 (dd, *J*=10.6, 3.5 Hz, 1H), 4.18 (q, *J*=7.1 Hz, 2H), 3.07 (d, *J*=9.7 Hz, 1H), 2.67 (br. s., 1H), 2.55 (dd, *J*=12.4, 3.6 Hz, 1H), 2.46 - 2.22 (m, 4H), 2.20 - 2.03 (m, 1H), 1.92 (t, *J*=10.3 Hz, 1H), 1.87 - 1.77 (m, 1H), 1.77 - 1.60 (m, 2H), 1.30 (t, *J*=7.2 Hz, 3H), 1.18 - 0.98 (m, 1H); HPLC t_r = 1.21 minutes (Method B).

Ethyl 2-((*R*)-1-((*S*)-2-(4-cyanophenyl)-2-hydroxyethyl)-piperidin-3-yl)acetate (15a) and ethyl 2-((*R*)-1-((*R*)-2-(4-cyanophenyl)-2-hydroxyethyl)-piperidin-3-yl)acetate (15b).[27]

Compound **15** was separated by chiral HPLC (Thar preparative SFC instrument) equipped with a Chiralpak AD-H (25 x 5 cm, 5 μm). Temp: 35°C; Flow rate: 270 mL/min; Mobile phase: CO_2/(MeOH + 0.1%DEA) in 3:1 ratio isocratic:

15a: Peak 1 (t_r = 5.5 min) was isolated (>99% d.e.). The hydroxyl stereochemistry of compound **15a** was assigned (*R,S*) because it matched (H-NMR and chiral HPLC retention) of material that was prepared using a chiral reducing agent precedented to generate this stereoisomer.[23] ^{1}H NMR (400 MHz, *CDCl$_3$*) δ ppm 7.63 (2 H, m), 7.48 (2 H, m, *J*=8.14 Hz), 4.75 (1 H, dd, *J*=10.67, 3.41 Hz), 4.15 (2 H, q, *J*=7.19 Hz), 3.04 (1 H, d, *J*=9.90 Hz), 2.65 (1 H, d, *J*=11.22 Hz), 2.52 (1 H, dd, *J*=12.54, 3.52 Hz), 2.18-2.43 (4 H, m), 2.04-2.18 (1 H, m, *J*=13.56, 6.81, 6.81, 3.63, 3.52 Hz), 1.88 (1 H, t, *J*=10.34 Hz), 1.75-1.84 (1 H, m), 1.59-1.74 (2 H, m), 1.24-1.31 (3 H, m), 1.00-1.15 (1 H, m); MS $(M+H)^+$ at *m/z* 317; HPLC purity: 95.4% with > 99% d.e.; t_r = 3.56 min. (Method: Chiralpak AD-H (0.46×25cm, 5μm). Temp: 40°C; Flow rate: 3 mL/min; Mobile phase: CO_2/ MeOH w 0.1%DEA in 7:3 ratio isocratic).

15b: Peak 2 (t_r = 7.0 min) was isolated (>99% d.e.). The hydroxyl stereochemistry of compound **15b** was assigned (*R,R*) based on the assignment of the other isomer. ^{1}H NMR (400 MHz, *CDCl$_3$*) δ ppm 7.63 (2 H, m), 7.48 (2 H, m, *J*=7.92 Hz), 4.75 (1 H, dd, *J*=10.56, 3.52 Hz), 4.14 (2 H, q, *J*=7.04 Hz), 3.00 (1 H, d, *J*=10.56 Hz), 2.72 (1 H, d, *J*=7.92 Hz), 2.51 (1 H, dd, *J*=12.32, 3.52 Hz), 2.32 (1 H, dd, *J*=12.43, 10.67 Hz), 2.20-2.26 (2 H, m), 2.01-2.20 (3 H, m), 1.70-1.85 (2 H, m), 1.52-1.68 (1 H, m), 1.26 (3 H, t, *J*=7.15 Hz), 1.00-1.13 (1 H, m); MS $(M+H)^+$ at *m/z* 317 ; HPLC purity: 94.1% with > 99% d.e.; t_r = 4.84 min. (Method: Chiralpak AD-H (0.46×25cm, 5μm). Temp: 40°C; Flow rate: 3 mL/min; Mobile phase: CO_2/ MeOH w 0.1%DEA in 7:3 ratio isocratic).

(*3S*)-ethyl-1-(2-hydroxy-2-(4-((Z)-N'-hydroxycarbamimidoyl)phenyl)ethyl)piperidine-3-carboxylate.[27]

To a mixture of **14** (2.34 g, 7.74 mmol) and hydroxylamine hydrochloride (1.076 g, 15.48 mmol) in 2-propanol (50 mL) was added sodium bicarbonate (2.60 g, 31.0 mmol). Heated at 80 °C overnight. The reaction mixture was diluted with ethyl acetate and washed with sat. NaCl. The organic layer was dried with $MgSO_4$, filtered and concentrated. Recovered 2.4 g of (*3S*)-ethyl-1-(2-hydroxy-2-(4-((Z)-N'-hydroxycarbamimidoyl)phenyl)ethyl)piperidine-3-carboxylate (92%). MS $(M+H)^+$ at *m/z* 336; HPLC t_r = 0.46 minutes (Method A).

(*3S*)-1-(2-hydroxy-2-(4-(5-(3-phenyl-4-(trifluoromethyl)isoxazol-5-yl)-1,2,4-oxadiazol-3-yl)phenyl)ethyl)piperidine-3-carboxylic acid (16).[27]

To a mixture of 3-phenyl-4-(trifluoromethyl)isoxazole-5-carbonyl fluoride (102 mg, 0.39 mmol) and (*3S*)-ethyl 1-(2-hydroxy-2-(4-((Z)-N'-hydroxycarbamimidoyl)phenyl)ethyl)piperidine-3-carboxylate (130 mg, 0.39 mmol) in CH_3CN (5 mL) was added DIEA (0.136 mL, 0.778 mmol). Stirred at rt for 2 hours. 1M TBAF in THF (0.389 mL, 0.389 mmol) was added and the reaction was stirred at rt overnight. The reaction mixture was diluted with ethyl acetate and washed with sat. NaCl. The organic layer was dried with $MgSO_4$, filtered and concentrated. To this product was added dioxane (2 mL) and 6N HCL (2 mL). The reaction mixture was gently warmed with a heat gun for a few minutes and then stirrred overnight at rt. The reaction mixture was filtered and purified by HPLC. HPLC conditions: Phenomenex Luna C18 5 μm column (250 x 30mm); 25-100% CH_3CN/water (0.1% TFA); 25 minute gradient; 30 mL/min. Isolated fractions with correct mass and freeze-dried overnight. Recovered 52 mg of (*3S*)-1-(2-hydroxy-2-(4-(5-(3-phenyl-4-(trifluoromethyl)isoxazol-5-yl)-1,2,4-oxadiazol-3-yl)phenyl)ethyl)piperidine-3-carboxylic acid, TFA salt (**16**, 20%) as a white solid. ^{1}H NMR (500MHz, *CD_3OD*) d 8.23 (d, J=8.5 Hz, 2H), 7.74 - 7.65 (m, 4H), 7.65 - 7.54 (m, 3H), 5.27 (dd, J=9.8, 4.5 Hz, 1H), 4.02 (d, J=11.8 Hz, 1H),

3.94 - 3.78 (m, 1H), 3.42 - 3.34 (m, 2H), 3.14 (dt, J=19.0, 12.5 Hz, 1H), 3.07 - 2.80 (m, 1H), 2.26 (d, J=12.6 Hz, 1H), 2.13 (d, J=15.4 Hz, 1H), 2.07 - 1.80 (m, 2H), 1.72 - 1.53 (m, 1H); MS $(M+H)^+$ at *m/z* 529; HPLC t_r = 3.23 minutes (Method B). HPLC purity: 99.2%; t_r = 8.70 min. (Method E).

ethyl 2-((*3R*)-1-(2-hydroxy-2-(4-((Z)-N'-hydroxycarbamimidoyl)phenyl)ethyl)piperidin-3-yl)acetate.[27]

To a mixture of **15** (356 mg, 1.125 mmol) and sodium bicarbonate (378 mg, 4.50 mmol) in 2-propanol (10 mL) was added hydroxylamine hydrochloride (156 mg, 2.250 mmol). Heated at 85 °C overnight. The reaction mixture was diluted with ethyl acetate and washed with water. The organic layer was dried with $MgSO_4$, filtered and concentrated. Recovered 346 mg of ethyl 2-((*3R*)-1-(2-hydroxy-2-(4-((Z)-N'-hydroxycarbamimidoyl)phenyl)ethyl)piperidin-3-yl)acetate (88%). MS $(M+H)^+$ at *m/z* 350; HPLC t_r = 1.06 minutes (Method B).

2-((*3R*)-1-(2-hydroxy-2-(4-(5-(3-phenyl-4-(trifluoromethyl)isoxazol-5-yl)-1,2,4-oxadiazol-3-yl)phenyl)ethyl)piperidin-3-yl)acetic acid (17).[27]

To a mixture of 3-phenyl-4-(trifluoromethyl)isoxazole-5-carbonyl fluoride (75 mg, 0.29 mmol) and ethyl 2-((*3R*)-1-(2-hydroxy-2-(4-((Z)-N'-hydroxycarbamimidoyl)phenyl)ethyl)piperidin-3-yl)acetate (98 mg, 0.29 mmol) in CH_3CN (5 mL) was added DIEA (0.102 mL, 0.583 mmol). Stirred at 25 °C for 3 hours. TBAF in THF (0.292 mL, 0.292 mmol) was added and the reaction was stirred at rt overnight. The reaction mixture was diluted with ethyl acetate and washed with sat. NaCl. The organic layer was dried with $MgSO_4$, filtered and concentrated. This product was dissolved in dioxane (2 mL) and 6N HCl was added. The reaction mixture was gently heated to solublize and then stirred overnight

at rt. The reaction mixture was filtered and purified by HPLC. HPLC conditions: Phenomenex Luna C18 5 μm column (250 x 30mm); 25-100% CH_3CN/water (0.1% TFA); 25 minute gradient; 30 mL/min. Isolated fractions with correct mass and freeze-dried overnight. Recovered 27mg of 2-((*3R*)-1-(2-hydroxy-2-(4-(5-(3-phenyl-4-(trifluoromethyl)isoxazol-5-yl)-1,2,4-oxadiazol-3-yl)phenyl)ethyl)piperidin-3-yl)acetic acid, TFA salt (**17,** 20%) as an off-white solid. ^{1}H NMR (500MHz, *CD_3OD*) δ 8.22 (d, J=8.35 Hz, 2H), 7.75 - 7.65 (m, 4H), 7.65 - 7.51 (m, 3H), 5.31-5.20 (m, 1H), 4.00-3.79 (m, 1H), 3.76 - 3.57 (m, 1H), 3.26 - 3.17 (m, 1H), 2.49-2.27 (m, 3H), 2.09-1.86 (m, 3H), 1.41 (sxt, J=7.38 Hz, 1H), 1.34-1.26 (m, 1H), 1.02(t J=7.36 Hz, 2H); MS $(M+H)^+$ at *m/z* 543; HPLC t_r = 3.23 minutes (Method B). HPLC purity: 99.2%; t_r = 8.81 min. (Method E).

(*S*)-1-((*S*)-2-hydroxy-2-(4-(5-(3-phenyl-4-(trifluoromethyl) isoxazol-5-yl)-1,2,4-oxadiazol-3-yl)phenyl)ethyl)piperidine-3-carboxylic acid (18a).[27]

To a mixture of **14a** (5.2 g, 17.2 mmol) and hydroxylamine hydrochloride (1.4 g, 20.6 mmol) in 2-propanol (50 mL) was added sodium bicarbonate (2.9 g, 84 mmol). The reaction mixture was heated at 85°C. The reaction mixture was diluted with EtOAc and washed with sat. NaCl. The organic layer was dried with $MgSO_4$, filtered, and concentrated to afford 5.35 g of (*S*)-ethyl 1-((*S*)-2-hydroxy-2-(4-((Z)-N'-hydroxycarbamimidoyl)phenyl)ethyl)piperidine-3-carboxylate (93%)

To a solution of 3-phenyl-4-(trifluoromethyl)isoxazole-5-carbonyl fluoride[21] (214 mg, 0.78 mmol) in CH_3CN (5 mL) was added DIEA (0.27 mL, 1.56 mmol) and (*S*)-ethyl-1-((S)-2-hydroxy-2-(4-((Z)-N'-hydroxycarbamimidoyl) phenyl) ethyl)piperidine-3-carboxylate (260 mg, 0.78 mmol). The reaction mixture was stirred for 2 hours, then 1M TBAF in THF (0.78 mL, 0.78 mmol) was added. The reaction mixture was stirred overnight at room temperature. The

reaction mixture was filtered and purified by HPLC in three batches. HPLC conditions: Phenomenex Luna C18 5 μm column (250 x 30mm); 25-100% CH_3CN/water (0.1% TFA); 25 minute gradient; 30 mL/min. Isolated fractions with correct mass were partitioned between EtOAc and saturated $NaHCO_3$. The aqueous layer was back extracted once. The combined organic layers were dried with $MgSO_4$, filtered, and concentrated to afford 155 mg of (*S*)-ethyl 1-((*S*)-2-hydroxy-2-(4-(5-(3-phenyl-4-(trifluoromethyl)isoxazol-5-yl)-1,2,4-oxadiazol-3-yl)phenyl)ethyl)piperidine-3-carboxylate (36%). ^{1}H NMR (400 MHz, *MeOH-d*$_3$) δ ppm 8.04 (2 H, d, *J*=8.13 Hz), 7.55-7.60 (2 H, m), 7.41-7.54 (5 H, m), 4.81 (1 H, ddd, *J*=8.35, 4.06, 3.84 Hz), 3.96-4.10 (2 H, m), 2.82-3.08 (1 H, m), 2.67-2.82 (1 H, m), 2.36-2.61 (3 H, m), 2.08-2.33 (2 H, m), 1.73-1.87 (1 H, m, *J*=8.54, 8.54, 4.45, 4.17 Hz), 1.32-1.70 (3 H, m), 1.09-1.19 (3 H, m). MS $(M+H)^+$ at *m/z* 557; HPLC purity: 99% t_r = 3.36 minutes (Method B).

(*S*)-ethyl 1-((*S*)-2-hydroxy-2-(4-(5-(3-phenyl-4-(trifluoromethyl)isoxazol-5-yl)-1,2,4-oxadiazol-3-yl)phenyl)ethyl)piperidine-3-carboxylate (35 mg, 0.063 mmol) was then heated at 50°C in 6N HCl (1 mL) and dioxane (1 mL). The reaction mixture was stirred overnight then filtered and purified by HPLC. HPLC conditions: Phenomenex Luna C18 5 μm column (250 x 30mm); 25-100% CH_3CN/water (0.1% TFA); 25 minute gradient; 30 mL/min. Isolated fractions with correct mass were freeze-dried overnight to afford 25 mg of (*S*)-1-((*S*)-2-hydroxy-2-(4-(5-(3-phenyl-4-(trifluoromethyl)isoxazol-5-yl)-1,2,4-oxadiazol-3-yl)phenyl)ethyl)piperidine-3-carboxylic acid, TFA salt (**18a**, 61%) as a white solid. ^{1}H NMR (400 MHz, *MeOH-d*$_3$) δ ppm 8.23 (2 H, d, *J*=8.35 Hz), 7.65-7.74 (4 H, m), 7.54-7.65 (3 H, m), 5.29 (1 H, t, *J*=7.03 Hz), 4.00 (1 H, br. s.), 3.43-3.75 (1 H, m), 3.34-3.41 (2 H, m), 2.82-3.24 (2 H, m), 2.26 (1 H, d, *J*=11.86 Hz), 1.84-2.14 (2 H, m), 1.52-1.75 (1 H, m); MS $(M+H)^+$ at *m/z* 529; HPLC t_r = 3.27 minutes (Method B). HPLC purity 99.4%; t_r = 8.78 min. (Method E); 99.0%; t_r = 7.29 min. (Method F);

This material was converted to the HCl salt for the following analyses: mp: 219.2 °C; Anal. Calcd for $C_{26}H_{23}N_4O_5F_3$•HCl, 0.14% water: C, 55.2; H, 4.31; N, 9.87; Cl, 6.25. Found: C, 55.39; H, 4.10; N, 9.88; Cl, 6.34. $[\alpha]_D^{20}$ +30.47 (*c* 0.336, MeOH); HPLC with chiral stationary phase (A linear gradient using CO_2 (Solvent A) and IPA with 0.1% DEA (Solvent B); *t* = 0 min., 30% B, *t* = 10 min., 55% B was employed on a Chiralcel AD-H 250 X 4.6 mm ID, 5 μm column. Flow rate was 2.0 ml/min); t_r = 5.38 min with >99% ee

(*S*)-1-((*R*)-2-hydroxy-2-(4-(5-(3-phenyl-4-(trifluoromethyl)isoxazol-5-yl)-1,2,4-oxadiazol-3-yl)phenyl)ethyl)piperidine-3-carboxylic acid (18b).[27]

Compound **18b** was synthesized by the same route as used for **18a** but using (*S*)-ethyl 1-((*R*)-2-(4-cyanophenyl)-2-hydroxyethyl)piperidine-3-carboxylate (**14b**) to give (*S*)-1-((*R*)-2-hydroxy-2-(4-(5-(3-phenyl-4-(trifluoromethyl)isoxazol-5-yl)-1,2,4-oxadiazol-3-yl)phenyl)ethyl)piperidine-3-carboxylic acid, TFA salt (**18b,** 23%) as a white solid. ^{1}H NMR (400 MHz, *MeOH-d*$_3$) δ ppm 8.14 (2 H, d, *J*=8.35 Hz), 7.57-7.66 (4 H, m), 7.44-7.56 (3 H, m), 5.17 (1 H, dd, *J*=9.67, 4.39 Hz), 3.65-4.02 (2 H, m), 3.25-3.46 (2 H, m), 2.77-3.13 (3 H, m), 1.98-2.29 (2 H, m), 1.70-1.91 (2 H, m), 1.42-1.64 (1 H, m). MS $(M+H)^+$ at *m/z* 529; HPLC t_r = 3.27 minutes (Method B); HPLC purity: 99.7%; t_r = 8.77 min. (Method E); 99.7%; t_r = 7.26 min. (Method F).

2-((R)-1-((S)-2-hydroxy-2-(4-(5-(3-phenyl-4-(trifluoromethyl)isoxazol-5-yl)-1,2,4-oxadiazol-3-yl)phenyl)ethyl)piperidin-3-yl)acetic acid (19a).[27]

To a mixture of **15a (**346 mg, 1.13 mmol) and sodium bicarbonate (378 mg, 4.5 mmol) in 2-propanol (10 mL) was added hydroxylamine hydrochloride (156 mg, 2.25 mmol). The reaction mixture was heated at 85°C overnight. The reaction mixture was diluted with EtOAc and washed with H_2O. The organic layer was dried with $MgSO_4$, filtered, and concentrated to

yield 346 mg of ethyl 2-((*3R*)-1-((*S*)-2-hydroxy-2-(4-((Z)-N'-hydroxycarbamimidoyl) phenyl)ethyl)piperidin-3-yl)acetate. MS $(M+H)^+$ at *m/z* 350; HPLC t_r = 1.02 minutes (Method A).

To a mixture of ethyl 2-((*3R*)-1-((*S*)-2-hydroxy-2-(4-((Z)-N'-hydroxycarbamimidoyl) phenyl)ethyl)piperidin-3-yl)acetate (198 mg, 0.57 mmol) and DIEA (0.198 mL, 1.1 mmol) in CH_3CN (10 mL) was added 3-phenyl-4-(trifluoromethyl)isoxazole-5-carbonyl fluoride. (147 mg, 0.57 mmol). The reaction mixture was stirred at room temperature. After 1 hr, 1M TBAF in THF (0.57 mL, 0.57 mmol) was added and the reaction mixture was stirred overnight. The reaction mixture was diluted with EtOAc and washed with H_2O. The organic layer was dried with $MgSO_4$, filtered, and concentrated. The resulting solids were purified on a silica gel cartridge using an EtOAc/hexanes gradient to afford ethyl 2-((*R*)-1-((*S*)-2-hydroxy-2-(4-(5-(3-phenyl-4-(trifluoromethyl)isoxazol-5-yl)-1,2,4-oxadiazol-3-yl)phenyl)ethyl)piperidin-3-yl)acetate. This product was then treated with 6N HCl/dioxane (1:1, 6 mL) at 50°C overnight. The reaction mixture was filtered and purified by HPLC. HPLC conditions: Phenomenex Luna C18 5 μm column (250 x 30mm); 25-100% CH_3CN/water (0.1% TFA); 25 minute gradient; 30 mL/min. Isolated fractions with correct mass were freeze-dried overnight to yield 107 mg of 2-((*R*)-1-((*S*)-2-hydroxy-2-(4-(5-(3-phenyl-4-(trifluoromethyl)isoxazol-5-yl)-1,2,4-oxadiazol-3-yl)phenyl)ethyl)piperidin-3-yl)acetic acid, TFA salt (**19a**, 28%, 2 steps) as a white solid. ^{1}H NMR (400 MHz, *MeOH-d*$_3$) δ ppm 8.13 (2 H, d, *J*=8.35 Hz), 7.57-7.64 (4 H, m), 7.44-7.55 (3 H, m), 5.17 (1 H, dd, *J*=9.23, 4.39 Hz), 3.81 (1 H, d, *J*=11.86 Hz), 3.56 (1 H, d, *J*=11.42 Hz), 3.24-3.31 (2 H, m), 2.82-2.95 (1 H, m), 2.72 (1 H, t, *J*=11.86 Hz), 2.16-2.40 (3 H, m), 1.79-1.95 (3 H, m), 1.10-1.34 (1 H, m); ^{13}C NMR (126 MHz, MeOD) δ ppm 174.69, 170.46, 165.65, 163.52, 156.94 (1 C, q, J=2.90 Hz), 146.62, 132.16, 130.19 (2 C, s), 130.00 (3 C, s), 129.08 (2 C, s),

128.15 (2 C, s), 127.49, 127.01, 121.91 (1 C, q, J=265.10 Hz), 113.84 (1 C, q, J=42.90 Hz), 68.14 (1 C, br. s.), 64.19 (1 C, br. s.), 56.95 (1 C, br. s.), 55.91 (1 C, br. s.), 38.49 (1 C, br. s.), 31.87 - 33.03 (1 C, m), 29.12, 23.85 (1 C, br. s.); MS $(M+H)^+$ at *m/z* 543; HPLC t_r = 3.26 minutes (Method B). HPLC purity 99.6%; t_r = 5.73 min. (Method E); 99.9%; t_r = 4.47 min. (Method F). This material was converted to the HCl salt for the following analyses: mp: 185.9 ^oC; Anal. Calcd for $C_{27}H_{25}N_4O_4F_3$ • 1.06 HCl, 0.26% water: C, 55.68; H, 4.54; N, 9.67; Cl, 6.59. Found: C, 55.51; H, 4.79; N, 9.45; Cl, 6.59; $[\alpha]_D^{20}$ +14.29 (*c* 0.319, MeOH); HPLC with chiral stationary phase (An isocratic run using 80% CO_2 (Solvent A) and 20% IPA with 0.1% DEA was employed on a Chiralcel AS-H 250 X 4.6 mm ID column. Flow rate was 2.0 ml/min); t_r = 4.29 min with >99.8% ee

2-((*R*)-1-((*R*)-2-hydroxy-2-(4-(5-(3-phenyl-4-(trifluoromethyl)isoxazol-5-yl)-1,2,4-oxadiazol-3-yl)phenyl)ethyl)piperidin-3-yl)acetic acid (19b).[27]

19b was synthesized by the same route as used for **19a** but using ethyl 2-((*R*)-1-((*R*)-2-(4-cyanophenyl)-2-hydroxyethyl)-piperidin-3-yl)acetate (**15b**) to give 2-((*R*)-1-((*R*)-2-hydroxy-2-(4-(5-(3-phenyl-4-(trifluoromethyl)isoxazol-5-yl)-1,2,4-oxadiazol-3-yl)phenyl)ethyl)piperidin-3-yl)acetic acid, TFA salt (**19b,** 41%) as a white solid. ^{1}H NMR (400 MHz, *MeOH-d*$_3$) δ ppm 8.14 (2 H, d, *J*=8.35 Hz), 7.57-7.63 (4 H, m), 7.45-7.56 (3 H, m), 5.16 (1 H, dd, *J*=8.79, 4.83 Hz), 3.54-3.81 (2 H, m), 2.83-2.97 (1 H, m), 2.66-2.78 (1 H, m), 2.64-2.96 (2 H, m), 2.14-2.46 (3 H, m), 1.67-2.02 (3 H, m), 1.11-1.42 (1 H, m). MS $(M+H)^+$ at *m/z* 543; HPLC t_r = 3.26 minutes (Method B). HPLC purity: 99.6%; t_r = 5.62 min. (Method E); 99.5%; t_r = 4.35 min. (Method F).

(*S*)-1-((*S*)-2-hydroxy-2-(4-(5-(3-(pyridin-2-yl)-4-(trifluoromethyl)isoxazol-5-yl)-1,2,4-oxadiazol-3-yl)phenyl)ethyl)piperidine-3-carboxylic acid (20a).[27]

To a mixture of 3-(pyridin-2-yl)-4-(trifluoromethyl)isoxazole-5-carboxylic acid[27] (45 mg, 0.174 mmol), (*S*)-ethyl 1-((*S*)-2-hydroxy-2-(4-((Z)-N'-hydroxycarbamimidoyl)phenyl)ethyl)piperidine-3-carboxylate (70 mg, 0.21 mmol), and BOP-Cl (53 mg, 0.21 mmol) in DMF (5 mL) was added TEA (0.073 mL, 0.52 mmol). The reaction mixture was stirred at room temperature for 2 hr then 1M TBAF (0.17 mL, 0.17 mmol) was added. Next, the reaction mixture was stirred for 3 days. The reaction mixture was diluted with EtOAc and washed with saturated NaCl. The organic layer was dried with $MgSO_4$, filtered, and concentrated. The crude residue was purified by a silica gel cartridge using an EtOAc/hexanes gradient to yield 37 mg of ethyl (*S*)-1-((*S*)-2-hydroxy-2-(4-(5-(3-(pyridin-2-yl)-4-(trifluoromethyl)isoxazol-5-yl)-1,2,4-oxadiazol-3-yl)phenyl)ethyl)piperidine-3-carboxylate (38%).

To a mixture of ethyl (*S*)-1-((*S*)-2-hydroxy-2-(4-(5-(3-(pyridin-2-yl)-4-(trifluoromethyl)isoxazol-5-yl)-1,2,4-oxadiazol-3-yl)phenyl)ethyl)piperidine-3-carboxylate (37 mg, 0.066 mmol) in CH_3CN (1ml) was added water (1 ml) and hydrochloric acid, 37% (1 ml). The reaction mixture was heated at 50°C overnight, then filtered and purified by HPLC. HPLC conditions: Phenomenex Luna C18 5 μm column (250 x 30mm); 20-100% CH_3CN/water (0.1% TFA); 25 minute gradient; 30 mL/min. Isolated fractions with correct mass were freeze-dried overnight to afford 30 mg of (*S*)-1-((*S*)-2-hydroxy-2-(4-(5-(3-(pyridin-2-yl)-4-(trifluoromethyl)isoxazol-5-yl)-1,2,4-oxadiazol-3-yl)phenyl)ethyl)piperidine-3-carboxylic acid, TFA salt (**20a,** 68%) as a pale yellow oil. ^{1}H NMR (400 MHz, *MeOH-d*$_3$) δ ppm 8.78 (1 H, d, *J*=4.39 Hz), 8.23 (2 H, d, *J*=8.35 Hz), 8.00-8.09 (1 H, m), 7.95 (1 H, d, *J*=7.91 Hz), 7.71 (2 H, d, *J*=8.35 Hz),

7.57-7.65 (1 H, m), 5.20-5.34 (1 H, m), 3.80-4.08 (1 H, m), 3.43-3.73 (1 H, m), 3.34-3.43 (2 H, m), 2.81-3.22 (3 H, m), 1.83-2.37 (4 H, m), 1.53-1.75 (1 H, m). MS $(M+H)^+$ at *m/z* 530; HPLC t_r = 2.80 minutes (Method B). HPLC purity: 97.6%; t_r = 7.68 min. (Method E); 97.1%; t_r = 6.73 min. (Method F).

2-((*R*)-1-((*S*)-2-hydroxy-2-(4-(5-(3-(pyridin-2-yl)-4-(trifluoromethyl)isoxazol-5-yl)-1,2,4-oxadiazol-3-yl)phenyl)ethyl)piperidin-3-yl)acetic acid (20b).[27]

3-(Pyridin-2-yl)-4-(trifluoromethyl)isoxazole-5-carboxylic acid[27] (40 mg, 0.16 mmol) was suspended in dichloromethane (1.5 mL) with sonication then DMF (5 µl, 0.065 mmol) was added. Oxalyl chloride (54 µl, 0.62 mmol) was added dropwise over 1-2 minutes. The reaction vial was flushed with argon and sealed. After 3 h, the contents were concentrated in vacuo. The material was re-constituted in dichloromethane and a solution of ethyl 2-((*3R*)-1-((*S*)-2-hydroxy-2-(4-((Z)-N'-hydroxycarbamimidoyl)phenyl)ethyl)piperidin-3-yl)acetate (54 mg, 0.16 mmol) in DCM (1-2 mL) was added. The reaction mixture was stirred for 3 days at room temperature and then purified by Prep HPLC to afford ethyl 2-((*R*)-1-((*S*)-2-hydroxy-2-(4-(5-(3-(pyridin-2-yl)-4-(trifluoromethyl)isoxazol-5-yl)-1,2,4-oxadiazol-3-yl)phenyl)ethyl)piperidin-3-yl)acetate which was suspended in dioxane (2-3 mL) and 3N aq HCl (1 mL) was added. The mixture was heated to 50°C overnight. The solution was evaporated and then placed under high vacuum to afford 10 mg of 2-((*R*)-1-((*S*)-2-hydroxy-2-(4-(5-(3-(pyridin-2-yl)-4-(trifluoromethyl)isoxazol-5-yl)-1,2,4-oxadiazol-3-yl)phenyl)ethyl)piperidin-3-yl)acetic acid, HCl (**20b,** 10%) as an off-white solid. ^{1}H NMR (500 MHz, *MeOD*) δ ppm 8.69 (1 H, d, *J*=4.72 Hz), 8.14 (2 H, d, *J*=8.32 Hz), 7.95 (1 H, td, *J*=7.70, 1.80 Hz), 7.86 (1 H, d, *J*=7.77 Hz), 7.61 (2 H, d, *J*=8.32 Hz), 7.49-7.56 (1 H, m), 5.17 (1 H, dd, *J*=9.71, 4.16 Hz), 3.80 (1 H, br. s.), 3.52-3.67 (4 H, m), 2.89 (1 H, br. s.), 2.73 (1 H, t,

J=11.93 Hz), 2.18-2.39 (3 H, m), 1.79-1.94 (3 H, m). HPLC t_r = 2.54 minutes (Method B). HPLC purity: 95.4%; t_r = 8.27 min. (Method E); 98.4%; t_r = 8.27 min. (Method F).

The following compounds were synthesized using the same routes as described above for **18a, 19a**, **20a** and **20b**.

(*S*)-1-((*S*)-2-hydroxy-2-(4-(5-(5-phenyl-4-(trifluoromethyl)isoxazol-3-yl)-1,2,4-oxadiazol-3-yl)phenyl)ethyl)piperidine-3-carboxylic acid (21a).[27]

Recovered 55 mg of (*S*)-1-((*S*)-2-hydroxy-2-(4-(5-(5-phenyl-4-(trifluoromethyl)isoxazol-3-yl)-1,2,4-oxadiazol-3-yl)phenyl)ethyl)piperidine-3-carboxylic acid, TFA salt (**21a**, 28%) as a white solid. ^{1}H NMR (400 MHz, *MeOD*) δ ppm 8.13 (2 H, d, *J*=8.36 Hz), 7.71 (2 H, d, *J*=7.48 Hz), 7.58-7.65 (3 H, m), 7.49-7.58 (2 H, m), 5.19 (1 H, t, *J*=6.93 Hz), 3.93 (1 H, d, *J*=11.44 Hz), 3.57 (1 H, d, *J*=12.54 Hz), 3.28 (2 H, d, *J*=6.82 Hz), 3.07 (1 H, t, *J*=12.21 Hz), 2.93 (1 H, td, *J*=12.54, 3.52 Hz), 2.81 (1 H, t, *J*=12.32 Hz), 2.17 (1 H, d, *J*=12.10 Hz), 1.86-2.06 (2 H, m), 1.45-1.64 (1 H, m, *J*=13.09, 12.82, 12.82, 3.74 Hz). MS $(M+H)^+$ at *m/z* 529; HPLC t_r = 3.19 minutes (Method B). HPLC purity: 97.7%; t_r = 7.67 min. (Method E); 98.3%; t_r = 6.47 min. (Method F).

2-((*R*)-1-((*S*)-2-hydroxy-2-(4-(5-(5-phenyl-4-(trifluoromethyl)isoxazol-3-yl)-1,2,4-oxadiazol-3-yl)phenyl)ethyl)piperidin-3-yl)acetic acid (21b).[27]

Recovered 66 mg of 2-((*R*)-1-((*S*)-2-hydroxy-2-(4-(5-(5-phenyl-4-(trifluoromethyl)isoxazol-3-yl)-1,2,4-oxadiazol-3-yl)phenyl)ethyl)piperidin-3-yl)acetic acid, TFA salt (**21b**, 19%) as a white solid. ^{1}H NMR (400 MHz, *MeOH-d_3*) δ ppm 8.12 (2 H, d, *J*=8.35 Hz), 7.71 (2 H, d, *J*=7.47 Hz), 7.49-7.66 (5 H, m), 5.16 (1 H, dd, *J*=9.67, 4.39 Hz), 3.81 (1 H, d, *J*=11.86 Hz), 3.56 (1 H, d, *J*=11.42 Hz), 3.14-3.33 (2 H, m), 2.83-2.94 (1 H, m), 2.72 (1

H, t, *J*=11.86 Hz), 2.16-2.38 (3 H, m), 1.78-1.92 (3 H, m), 1.10-1.33 (1 H, m). MS $(M+H)^+$ at *m/z* 543; HPLC t_r = 3.24 minutes (Method B). HPLC purity: 99.5%; t_r = 7.66 min. (Method E); 100%; t_r = 6.43 min. (Method F).

(*S*)-1-((*S*)-2-hydroxy-2-(4-(5-(5-isobutyl-4-(trifluoromethyl)isoxazol-3-yl)-1,2,4-oxadiazol-3-yl)phenyl)ethyl)piperidine-3-carboxylic acid (22a).[27]

Recovered 24 mg of (*S*)-1-((*S*)-2-hydroxy-2-(4-(5-(5-isobutyl-4-(trifluoromethyl)isoxazol-3-yl)-1,2,4-oxadiazol-3-yl)phenyl)ethyl)piperidine-3-carboxylic acid (**22a,** 52%) as a tan solid. ^{1}H NMR (400 MHz, *MeOD*) δ ppm 8.19 (2 H, d, *J*=8.36 Hz), 7.70 (2 H, d, *J*=8.36 Hz), 5.26 (1H, dd, *J*=10.45, 2.97 Hz), 3.25-3.40 (6 H, m), 3.02 (2 H, dd, *J*=7.26, 1.10 Hz), 2.80-2.88 (1 H, m), 2.14-2.26 (1 H, m), 1.89-2.08 (4 H, m), 1.05 (3 H, s), 1.04 (3 H, s). MS $(M+H)^+$ at *m/z* 509; HPLC t_r = 3.78 minutes (Method B). HPLC purity: 98.9%; t_r = 8.71 min. (Method E); 98.7%; t_r = 7.71 min. (Method F).

2-((*R*)-1-((*S*)-2-hydroxy-2-(4-(5-(5-isobutyl-4-(trifluoromethyl)isoxazol-3-yl)-1,2,4-oxadiazol-3-yl)phenyl)ethyl)piperidin-3-yl)acetic acid (22b).[27]

Recovered 17 mg of 2-((*R*)-1-((*S*)-2-hydroxy-2-(4-(5-(5-isobutyl-4-(trifluoromethyl)isoxazol-3-yl)-1,2,4-oxadiazol-3-yl)phenyl)ethyl)piperidin-3-yl)acetic acid, TFA salt (**22b**, 15%) as a clear oil. ^{1}H NMR (400 MHz, *MeOD*) δ ppm 8.09 (2 H, m, *J*=8.36 Hz), 7.58 (2 H, d, *J*=8.36 Hz), 5.16 (1 H, dd, *J*=9.24, 4.62 Hz), 3.80 (1 H, d, *J*=11.22 Hz), 3.57 (1 H, d, *J*=13.42 Hz), 2.91 (2 H, dd, *J*=7.26, 1.10 Hz), 2.79 - 2.90 (1 H, m), 2.73 (1 H, t, *J*=11.77 Hz), 2.18 - 2.39 (3 H, m), 2.09 (1 H, dt, *J*=13.64, 6.82 Hz), 1.82 - 1.93 (3 H, m), 1.14 - 1.31 (1 H, m), 0.94 (6 H, d, *J*=6.60 Hz). MS $(M+H)^+$ at *m/z* 523; HPLC t_r = 3.28 minutes (Method B). HPLC purity: 97.9%; t_r = 8.95 min. (Method E); 96.7%; t_r = 7.83 min. (Method F).

2-((*R*)-1-((*S*)-2-(4-(5-(5-cyclohexyl-4-(trifluoromethyl)isoxazol-3-yl)-1,2,4-oxadiazol-3-yl)phenyl)-2-hydroxyethyl)piperidin-3-yl)acetic acid (23).[27]

Recovered 15 mg of 2-((*R*)-1-((*S*)-2-(4-(5-(5-cyclohexyl-4-(trifluoromethyl)isoxazol-3-yl)-1,2,4-oxadiazol-3-yl)phenyl)-2-hydroxyethyl)piperidin-3-yl)acetic acid, HCL (**23**, 21%) as a pale yellow solid. ^{1}H NMR (400 MHz, *MeOD*) δ ppm 8.09 (2 H, d, *J*=8.36 Hz), 7.59 (2 H, d, *J*=8.36 Hz), 5.13 - 5.22 (1 H, m), 3.80 (1 H, d, *J*=10.56 Hz), 3.53 - 3.62 (2 H, m), 2.91 (1 H, br. s.), 2.75 (1 H, t, *J*=11.44 Hz), 2.17 - 2.39 (3 H, m), 1.79 - 1.97 (7 H, m), 1.58 - 1.78 (3 H, m), 1.19 - 1.44 (4 H, m). MS $(M+H)^+$ at *m/z* 549; HPLC t_r = 3.52 minutes (Method B). HPLC purity: 96.8%; t_r = 9.71 min. (Method E).

ASSOCIATED CONTENT

Supporting Information Available.

The Supporting Information is available free of charge on the ACS Publications website.

X-ray crystallographic structure of **14a** (PDF,PDB)

Docking of **19a** into the crystal structure of $S1P_1$ in complex with ML056 (PDB)

Molecular formula strings (CSV)

AUTHOR INFORMATION

* To whom correspondence should be addressed. Phone: 609-252-3153. E-mail: john.gilmore@bms.com.

ABBREVIATION USED

[a] Abbreviations: S1P, Sphingosine-1-phosphate; $S1P_{1-5}$, Sphingosine-1-phosphate receptors 1-5; BLR, rat blood lymphocyte reduction; TM, transmembrane; AA, adjuvant induced arthritis; EAE, experimental autoimmune encephalomyelitis.

REFERENCES

(1) Billich, A.; Bornancin, F.; Devay, P.; Mechtcheriakova, D.; Urtz,N.; Baumruker, T. Phosphorylation of the immunomodulatory drug FTY720 by sphingosine kinases. *J. Biol. Chem*. **2003**, *278*, 47408−47415.

(2) Albert, R.; Hinterding, K.; Brinkmann, V.; Guerini, D.; Muller-Hartwieg, C.; Knecht, H.; Simeon, C.; Streiff, M.; Wagner, T.;Welzenbach, K.; Ze´cri, F.; Zollinger, M.; Cooke, N.; Francotte, E. Novel immunomodulator FTY720 is phosphorylated in rats and humans to form a single stereoisomer. identification, chemical proof, and biological characterization of the biologically active species and its enantiomer. *J. Med. Chem*. **2005**, *48*, 5373−5377.

(3) Chun, J.; Hartung, H. Mechanism of action of oral fingolimod (FTY720) in multiple schlerosis. *Clin. Neuropharmacol.* **2010**, *33*, 91-101.

(4) Mandala, S.; Hajdu, R.; Bergstrom, J.; Quackenbush, E.; Xie, J.; Milligan, J.; Thornton, R.; Shei, G-J.; Card, D.; Keohane, CA.; Rosenbach, M.; Hale, J.; Lynch, C. L.; Rupprecht, K.; Parsons, W.; Rosen, H. Alteration of lymphocyte trafficking by sphingosine-1-phosphate receptor agonists. *Science* **2002**, *296*, 346-349.

(5) Brinkmann, V.; Davis, M. D.; Heise, C. E.; Albert, R.; Cottens, S.; Hof, R.; Bruns, C.; Prieschl, E.; Baumruker, T.; Hiestand, P.; Foster, C. A.; Zollinger, M.; Lynch, K. R. The immune modulator FTY720 targets sphingosine 1-phosphate receptors. *J. Biol. Chem*.

2002, *277*, 21453-21457.

(6) Cyster, J. G.; Schwab, S. R. Sphingosine-1-phosphate and lymphocyte egress from lymphoid organs *Annu. Rev. Immunol*. **2012**. *30*, 69–94.

(7) (a) Hla, T.; Vendataraman, K.; Michaud, J. The vascular S1P gradient: cellular sources and biological significance. *Biochim. Biophys. Acta* **2008**, *1781*, 477-482. (b) Schwab, S. R.; Cyster, J. G. Finding a way out: lymphocyte egress from lymphoid organs. *Nat. Immunol.* **2007**, *8*, 1295-1301. (c) Rosen, H.; Goetzl, E. J. Sphingosine 1-phosphate and its receptors: an autocrine and paracrine network. *Nat. Rev. Immunol*. **2005**, *5*, 560-570.

(8) Pappu, R.; Schwab, S. R.; Cornelissen, I.; Pereira, J. P.; Regard, J. B.; Xu, Y.; Camerer, E.; Zheng, Y.-W.; Huang, Y.; Cyster, J. G.; Coughlin, S. R. Promotion of lymphocyte egress into blood and lymph by distinct sources of sphingosine-1-phosphate. *Science* **2007**, *316*, 295–298.

(9) Singer, B.; Ross A. P.; Tobias, K. Oral fingolomid for the treatment of patients with relapsing forms of multiple sclerosis. *Int. J. Clin. Pract*. **2011**, *65*, 887-895.

(10) Sanchez, T.; Estrada-Hernandez, T.; Paik, J-H.; wu, M-T.; Venkataraman, K.; Brinkmann, V.; Claffey, K.; Hla, T. Phosphorylation and action of the immunomodulatory FTY720 inhibits vascular endothelial cell growth factor-induced vascular permeability. *J Biol. Chem.* **2003**, *47*, 47281-47290.

(11) Kappos, L.; Antel, J.; Comi, G.; Montalban, X.; O'Connor, P.; Polman, C. H.; Haas, T.; Korn, A. A.; Karlsson, G.; Radue, E. W. Oral fingolimod (FTY720) for relapsing multiple sclerosis. *N. Engl. J. Med*. **2006**, *355*, 1124-1140.

(12) Sanna, M.G.; Liao, J.; Jo, E., Alfonso, C.; Ahn, M.-Y.; Peterson, M.S.; Webb, B.; Rosen, H. Sphingosine 1-phosphate (S1P) receptor subtypes $S1P_1$ and $S1P_3$, respectively, regulate lymphocyte recirculation and heart rate. *J. Biol. Chem.* **2004**, *279*, 13839-13848.

(13) Forrest, M.; Sun, S.-Y.; Hajdu, R.; Bergstrom, J.; Card, D.; Doherty, G.; Hale, J.; Keohane, C.; Meyers, C.; Milligan, J.; Mills, S.; Nomura, N.; Rosen, H.; Rosenbach, M.; Shei, G.-J.; Singer, I. I.; Tian, M.; West, S.; White, V.; Xie, J.; Proia, R. L.; Mandala, S. Immune cell regulation and cardiovascular effects of sphingosine 1-phosphate receptor agonists in rodents are mediated via distinct receptor subtypes. *J. Pharmacol. Exp. Ther*. **2004**, *309*, 758–768.

(14) Li, Z.; Chen, W.; Hale, J. J.; Lynch, C. L.; Mills, S. G.; Hajdu, R.; Keohane, C. A.; Rosenbach, M. J.; Milligan, J. A.; Shei, G-J.; Chrebet, G.; Parent, S. A.; Bergstrom, J.; Card, D.; Forrest, M.; Quackenbush, E. J.; Wickham, L. A.; Vargas, H.; Evans, R. M.; Rosen, H.; Mandala, S. Discovery of potent 3,5-diphenyl-1,2,4-oxadiazole sphingosine-1-phosphate-1 ($S1P_1$) receptor agonists with exceptional selectivity against $S1P_2$ and $S1P_3$. *J. Med. Chem*. **2005**, *48*, 6169-6173.

(15) (a) Buzard, D. J.; Schrader, O.; Zhu, X.; Lehmann, J.; Johnson, B.; Kasem, M.; Kim, S.-H.; Kawasaki, A.; Lopez, L.; Moody, J.; Han, S.; Gao, Y.; Edwards, J.; Barden, J.; Thatte, J.; Gatlin, J.; Jones, R. M. Design and synthesis of new trycyclic indoles as potent modulators of the S1P1 receptor. *Bioorg. Med. Chem. Lett*. **2015**, *25*, 659-663. (b) Buzard, D. J.; Lopez, L.; Moody, J.; Kawasaki, A.; Schrader, T. O.; Kasem, M.; Johnson, B.; Zhu, X.; Thoresen, L.; Kim, S. H.; Gharbaoui, T.; Sengupta, D.; Calvano, L.; Krishnan, A.; Gao, Y.; Semple, G.; Edwards, J.; Barden, J.; Morgan, M.; Usmani, K.; Chen, C.; Sadeque, A.; Chen, W.; Christopher, R. J.; Thatte, J.; Fu, L.; Solomon, M.;

Whelan, K.; Al-Shamma, H.; Gatlin, J.; Gaidarov, I.; Anthony, T.; Le, M.; Unett, D. J.; Stirn, S.; Blackburn, A.; Behan, D. P.; Jones, R. M. (7-Benzyloxy-2,3-dihydro-1H-pyrrolo[1,2-a]indol-1-yl)acetic acids as S1P1 functional agonists. *Med. Chem. Lett*. **2014**, *5*, 1334-1339. (c) Skidmore, J.; Heer, J., Jhonson, C. N.; Norton, D.; Redshaw, S.; Sweeting, J.; Hurst, D.; Cridland, A.; Vesey, D.; Wall, I.; Ahmed, M.; Rivers, D.; Myatt, J.; Giblin, G.; Philpott, K.; Kumar, U.; Stevens, A.; Bit, R. A.; Haynes, A.; Taylor, S.; Watson, R.; Witherington, J.; Demont, E.; Heightman, T. D. Optimization of sphingosine-1-phosphate receptor agonists: effects of acidic, basic, and zwitterionic chemotypes on pharmacokinetic and pharmacodynamics profiles. *J. Med. Chem*. **2014**, *57*, 10424-10442. (d) Bolli, M. H.; Abele, S.; Birker, M.; Brave, R.; Bur, D.; de Kanter, R.; Kohl, C.; Grimont, J.; Hess, P.; Lescop, C.; Mathys, B.; Muller, C.; Nayler, O.; Rey, M.; Scherz, M.; Schmidt, G.; Seifert, J.; Steiner, B.; Velker, J.; Weller, T. Novel S1P1 receptor agonists – part 3: from thiophenes to pyridines. *J. Med. Chem*. **2014**, *57*, 110-130. (e) Bolli, M. H.; Velker, J.; Muller, C.; Mathys, B.; Birker, M.; Bravo, R.; Bur, D.; de Kanter, R.; Hess, P.; Kohl, C.; Lehmann, D.; Meyer, S.; Nayler, O.; Rey, M; Scherz, M.; Steiner, B. Novel S1P1 receptor agonists – part 2: from bicylco[3.1.0]hexane-fused thiophenes to isobutyl substituted thiophenes. *J. Med. Chem.* **2014**, *57*, 78-97. (f) Horan, J. C.; Sanyal, S.; Choi, Y.; Hill-Drzewi, M.; Patnaude, L.; Anderson, S.; Fogal, S.; Mao, C.; Cook, B. N.; Gueneva-Boucheva, K.; Fisher, M. B.; Hickey, E.; Pack, E.; Bannen, L. C.; Chan, D. S.; Mac, M. B.; Ng, S. M.; Wang, Y.; Xu, W.; Modis, L. K.; Lemieux, R. M. Piperazinyl-oxadiazoles as selective sphingosine-1-phosphate receptor agonists. *Bioorg. Med. Chem. Lett.* **2014**, *24*, 4807-4811.

(16) (a) Dyckman, A. Recent advances in the discovery and development of sphingosine-1-phosphate-1 receptor agonists *Ann. Rep. Med. Chem.* **2012** 195-207 and references cited therein. (b) Roberts, E.; Guerrero, M.; Urbano, M.; Rosen, H. Sphingosine 1-phosphate receptor agonists: a patent review (2010-2012). *Expert Opin. Ther. Pat.* **2013** *23*, 7 817-841 and references cited therein.

(17) Blaho, V. A.; Hla, T. An update on the biology of sphingosine 1-phosphate receptors. *J. Lipid Res.* **2014** *55*, 1596–1608.

(18) Gergely, P.; Nuesslein-Hildesheim, B.; Guerini, D.; Brinkmann, V.; Traebert, M.; Bruns, C.; Pan, S.; Gray, N. S.; Hinterding, K.; Cooke, N. G.; Groenewegen, A.; Vitaliti, A.; Sing, T.; Luttringer, O.; Yang, J.; Gardin, A.; Wang, N.; Crumb, W. J. Jr.; Saltzman, M.; Rosenberg, M.; Wallstrom, E. The selective sphingosine 1-phosphate receptor modulator BAF312 redirects lymphocyte distribution and has species-specific effects on heart rate. *Br. J. Pharm*. **2012**, *167*, 1035-1047.

(19) David, O. J.; Kovarik J. M,; Schmouder R. L. Clinical pharmacokinetics of fingolimod. *Clin. Pharmacokinet*. **2012**, *51*, 15−28.

(20) (a) Hale, J. J.; Lynch, C. L.; Neway, W.; Mills, S. G.; Hajdu, R.; Keohane, C. A.; Rosenbach, M. J.; Milligan, J. A.; Shei, G. J.; Parent, S. A.; Chrebet, G.; Bergstrom, J.; Card, D.; Ferrer, M.; Hodder, P.; Strulovici, B.; Rosen, H.; and Mandala, S. A rational utilization of high-throughput screening affords selective, orally bioavailable 1- benzyl-3-carboxyazetidine sphingosine-1-phosphate-1 receptor agonists. *J. Med. Chem.* **2004**, *47*, 6662−6665. (b) Pan, S.; Gray, N-S.; Gao, W.; Mi, Y.; Fan, Y.; Wang, X.; Tuntland, T.; Che, J.; Lefebvre, S.; Chen, Y.; Chu, A.; Hinterding, K.; Gardin, A.; End, P.; Heining, P.; Bruns, C.; Cooke, N.G.; and Nuesslein-Hildesheim, B. Discovery of BAF312

(siponimod), a potent and selective S1P receptor modulator *ACS Med. Chem. Lett*. **2013**, *4*, 333–337. (c) Lanman, B. A.; Cee, V. J.; Cheruku, S. R.; Frohn, M.; Golden, J.; Lin, J.; Lobera, M; Marantz, Y.; Muller, K. M.; Neira, S. C.; Pickrell, A. J.; Rivenzon-Segal, D.; Nili Schutz, N.; Anurag Sharadendu, A.; Xiang Yu, X.; Zhaoda Zhang, Z.; Janet Buys, J.; Fiorino, M.; Gore, A.; Horner, M.; Itano, A.; McElvain, M.; Middleton, S.; Schrag, M.; Vargas, H. M.; Xu, H.; Xu, Y.; Zhang, X.; Siu, J.; and Bürli, R. W. Discovery of a potent, S1P3-sparing benzothiazole agonist of sphingosine-1-phosphate receptor 1 (S1P1) *ACS Med. Chem. Lett.*, **2011**, *2*, 102–106. (d) Ren, F.; Deng, G.; Wang, H.; Luan, L.; Meng, Q.; Xu, Q.; Xu, H.; Xu, X.; Zhang, H.; Zhao, B.; Li, C.; Guo, T. B.; Yang, J.; Zhang, W.; Zhao, Y.; Jia, Q.; Lu, H.; Xiang, J-N.; Elliott, J. D.; Lin, X. Discovery of novel 1,2,4-thiadiazole derivatives as potent, orally active agonists of sphingosine 1-phosphate receptor subtype 1 (S1P1) *J.Med. Chem*. **2012** , *55*, 4286 – 4296. (e) Cee, V. J.; Frohn, M.; Lanman, B. A.; Golden, J.; Muller, K.; Neira, S.; Pickrell, A.; Arnett, H.; Buys, J.; Gore, A.; Fiorino, M.; Horner, M.; Itano, A.; Lee, M. R.; McElvain, M.; Middleton, S.; Schrag, M.; Rivenzon-Segal, D.; Vargas, H. M.; Xu, H.; Xu, Y.; Zhang, X.; Siu, J.; Wong, M.; Buerli, R. W. Discovery of AMG 369, a thiazolo[5,4-b]pyridine agonist of S1P1 and S1P5. *ACS Med. Chem. Lett*. **2011**, *2*, 107 – 112.

(21) (a) Watterson, S. H.; Guo, J.; Spergel, S. H.; Langevine, C. M.; Moquin, R. V.; Shen, D. R.; Yarde, M.; Cvijic, M. E.; Banas, D.; Liu, R.; Suchard, S. J.; Gillooly, K.; Taylor, T.; RexRabe, S.; Shuster, D. J.; McIntyre, K. W.; Cornelius, G.; Darienzo, C.; Marino, A.; Balimane, P.; Warrick, B.; Saltercid, L.; McKinnon, M.; Barrish, J. C.; Carter, P. C.; Pitts, W. J.; Xie, J.; Dyckman, A. J. Potent and selective agonists of sphingosine-1-phosphate 1 ($S1P_1$): the discovery and SAR of a novel isoxazole based series. *J. Med.*

*Che*m. **2016**, *59*, 2820-2840. (b) Watterson, S. H.; Dyckman, A. J.; Pitts, W. J.; Spergel, S. H. Substituted isoxazole derivatives as S1P agonists in the treatment of autoimmune and inflammatory diseases and their preparation. WO 2010085581; *Chem. Abstr*. 2010, *153*, 232588 (US Patent 8354398 2013).

(22) The absolute and relative stereochemistry of compound **14a** was unambiguously assigned (*S,S*) by X-ray crystal structure**.** Crystallographic data for the structures **14a** reported in this paper has been deposited with the Cambridge Crystallographic Data Centre as supplementary publication nos. CCDC 1452864. Copies of the data can be obtained free of charge on application to CCDC, 12 Union Road, Cambridge CB2 1EZ, UK (fax: (‡44) 1223-336-033; e-mail: deposit@ccdc.cam.ac.uk). The absolute and relative stereochemistry of **14b** was assigned (*S,R*) based on the crystal structure of **14a.**

(23) The stereochemical assignment of **15a** was made by preparation of the material using the procedures described in WO2009005646. The starting (2-bromoacetyl)benzonitrile was reduced with (*S*)-2-methyl-CBS-oxazaborolidine followed by BH_3-SMe_2 yielding a 10:1 mixture of the *S:R* isomer. Subsequent HPLC chiral separation removed the minor isomer and coupling with the commercially available (*R*)-ethyl 2-(piperidin-3-yl)acetate afforded **15a** which was assigned as the (*R,S*) isomer.

(24) Hanson, M.A.; Roth, C.B.; Jo, E.; Griffith, M.T.; Scott, F.L.; Reinhart, G; Desale, H; Clemons, B.; Cahalan, S.M.; Schuerer, S.C.; Sanna, M.G.; Han, G.W.; Rosen, H; Stevens, R.C. Crystal structure of a lipid G-protein coupled receptor. *Science* **2012**, *335*, 851-855.

(25) The des-hydroxy version of **11l** was prepared and this resulted in >380 fold loss of activity in the $S1P_1$ binding assay. Additionally, the methoxy version of **11b** resulted in a >700 fold loss of activity in the $S1P_1$ binding assay.

(26) Bendele, A.; McComb, J.; Gould, T.; McAbee, T.; Sennello, G.; Chlipala, E.; Guy, M. Animal models of arthritis: relevance to human disease. *Toxicol. Pathol.* **1999**, *27*, 134-142.

(27) Gilmore, John L.; Sheppeck, James E; Sphingosine-1-phosphate receptor agonists. WO201117578, *Chem. Abstr.* **2011**, *154*, 259630, (US Patent 8399451 **2013**).

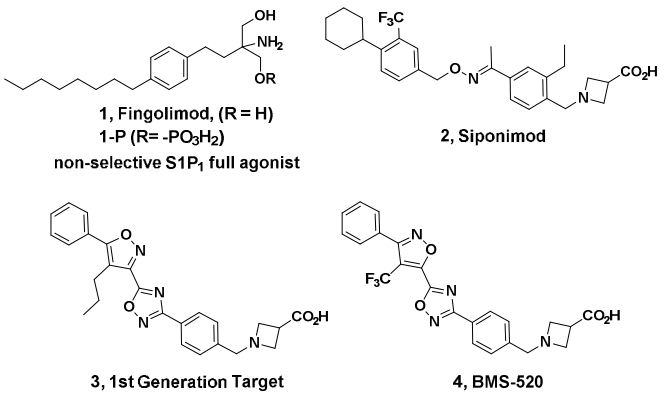

Figure 1.

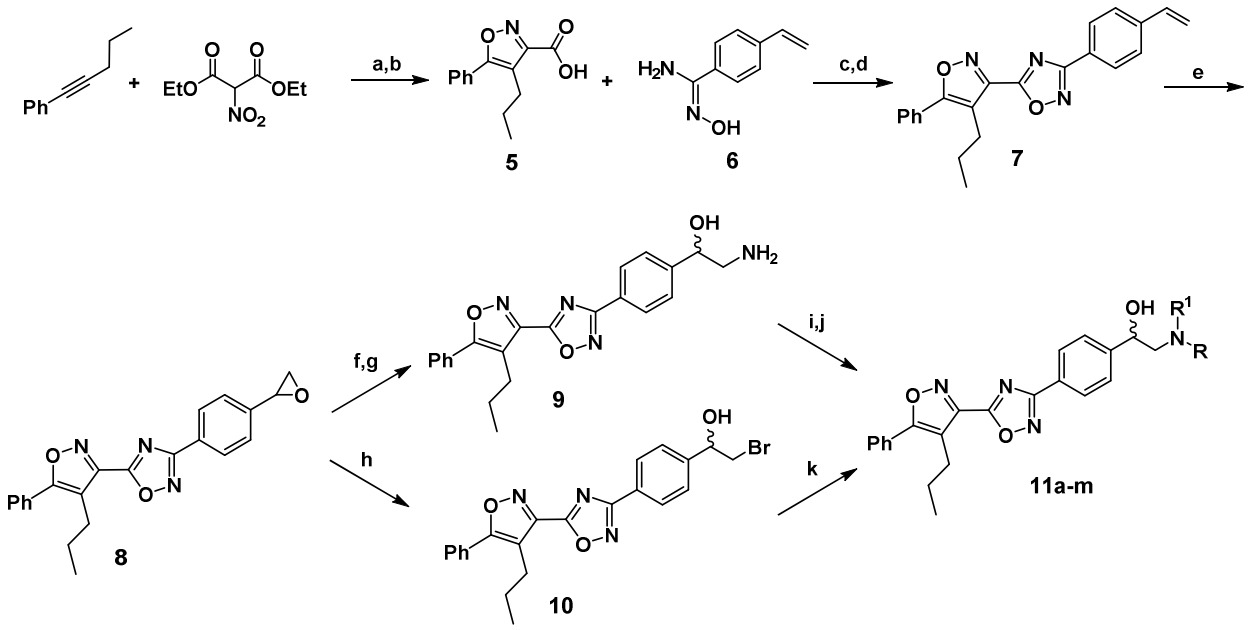

Scheme 1[a]: Synthesis of Propylisoxazole Ethanolamines

[a] Reagents and conditions: (a) 160 °C, 18h, 87%; (b) 1M NaOH, EtOH, 75 °C, 12h, 95%; (c) cyanuric fluoride, pyridine, DCM, rt, 1h, 90%; (d) DIEA, CH_3CN, rt then heat at 70 °C, 18 h, 45%; (e) m-CPBA, DCM, rt, 12h, 62%; (f) phthalimide, cat. potassium phthalimide, 100 °C, 12h, 85%; (g) $NH_2NH_2{\cdot}H_2O$, EtOH, 75 °C, 35%; (h) bromotriethylsilane, THF, -78 °C, 2h, 50%; (i) R-Br, NaI, pyridine, 80 °C; (j) 6N HCl, EtOH or MeOH, 70 °C, 12h, 95% or TFA/DCM (1:1); (k) RR'-NH, DBU or tetrabutylammonium hydroxide, DMSO, 80 °C, 10-50%.

Table 1. SAR of Propylisoxazole Ethanolamines

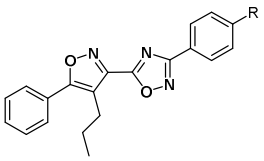

Compds	R	$S1P_1$ binding IC_{50}, nM	$S1P_1$ GTPγS EC_{50}, nM (Ymax)	$S1P_3$ GTPγS EC_{50}, nM (Ymax)	Compds	R	$S1P_1$ binding IC50, nM	$S1P_1$ GTPγS EC_{50}, nM (Ymax)	$S1P_3$ GTPγS EC_{50}, nM (Ymax)
9		1.5[b]	64 (95)[b]	nt	**11g**	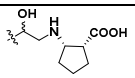	0.51[a]	27 (104)[a]	1100 (100)[b]
11a	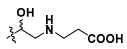	0.13[b]	38 (86)[b]	2500 (90)[a]	**11h**	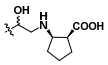	1.8[a]	nt	2100 (80)[a]
11b	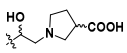	0.69[a]	61 (96)[a]	nt	**11i**	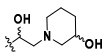	13[a]	128 (93)[a]	5600 (137)[a]
11c	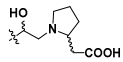	36[a]	230 (76)[a]	3800 (89)[a]	**11j**	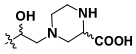	9.4[a]	95 (85)[a]	20300 (67)[a]
11d		7.0[a]	110 (96)[a]	1300 (100)[a]	**11k**	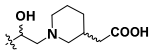	nt	11 (86)[a]	900 (88)[a]
11e	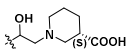	1.0±0.6[c]	6.9 (86)[b]	2000 (100)[a]	**11l**	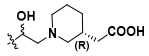	0.21[a]	3.9 (86)[a]	1200 (100)[a]
11f	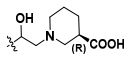	25[a]	170 (102)[a]	21000 (117)[a]	**11m**	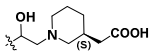	4.0[a]	34 (91)[a]	>31300[a]

[a] IC_{50}/ EC_{50} values are shown as single determinations; [b] IC_{50}/EC_{50} values are shown as a mean of two determinations;
[c] IC_{50}/EC_{50} values are shown as a mean of at least three determinations; nt = not tested

Table 2. Effects of select propylisoxazole ethanolamines on blood lymphocyte counts in Lewis rats (n = 3)

Compds	Dose (mg/kg)	Lymphoyte Red,. 4h (Exposure, nM)[b]	Lymphoyte Red, 24h (Exposure, nM)[b]
11a	30	-74% (142)	-11% (LLQ)[a]
11e	10	-77% (1595)	-5.3% (38)
11l	3	-81% (685)	-25% (40)

[a] LLQ = below detectable limits. [b] Exposure: plasma concentration at the time indicated

Scheme 2 [a]: Synthesis of Trifluoromethyloxazole Ethanolamines

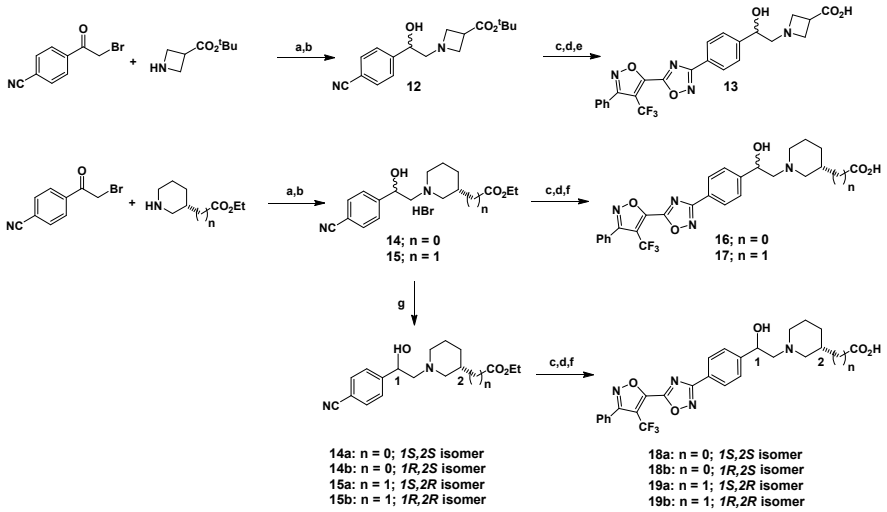

[a] Reagents and conditions: (a) toluene, rt, 18h; (b) $NaBH_4$, EtOH or MeOH, 80-95% (c) NH_2OH, $NaHCO_3$, ^iPrOH 85-90%; (d) 3-Phenyl-4-(trifluoromethyl)isoxazole-5-carbonyl fluoride, DIEA, CH_3CN, rt, 2h then TBAF/THF, 12h, 20-50%; (e) TFA/ CH_2Cl_2 (1:1) (f) 6N HCl, CH_3CN or dioxane, 80 ^oC, 12h, 80 %; (g) Chiral HPLC separation of isomers.

Table 3. SAR of Trifluromethyloxazole Ethanolamines

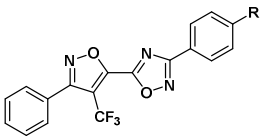

Compds	R	$S1P_1$ binding IC_{50}, nM[a]	$S1P_1$ GTPγS EC_{50}, nM[a] (Ymax)	$S1P_3$ GTPγS EC_{50}, nM[a] (Ymax)	Rat BLR[d] % lymphocyte reduction, 24h (dose)
13	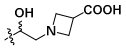	5.8[a]	7.8 (98)[a]	12000 (69)[a]	-70% (3 mpk)
16	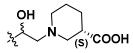	0.47[b]	7.8±3.5[c]	14000 (85)[c]	-81% (3 mpk)
17	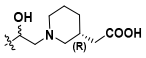	0.11[b]	4.2±1.0[c]	3500 (100)[a]	-75% (1 mpk)

[a] IC_{50}/ EC_{50} values are shown as single determinations; [b] IC_{50}/EC_{50} values are shown as a mean of two determinations; [c] IC_{50}/EC_{50} values are shown as a mean of at least three determinations; [d]Compounds tested in Lewis rat (n = 3)

Table 4. SAR of Homochiral Trifluoromethyloxazole Ethanolamines

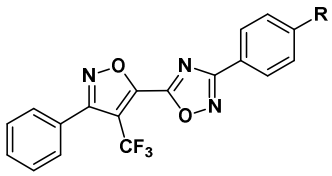

Compds	R	$S1P_1$ GTPgS EC_{50}, nM[a] (Ymax)	$S1P_3$ GTPgS EC_{50}, nM[a] (Ymax)	$S1P_4$ GTPgS EC_{50}, nM[b] (Ymax)	$S1P_5$ GTPgS EC_{50}, nM[b] (Ymax)
18a	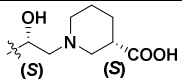	3.5±1.5 (98)	9400±5200 (87)	0.92 (89)	1.1 (87)
18b	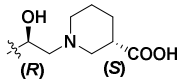	30±9 (102)	12,000±9200 (100)	nt	nt
19a	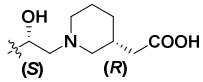	1.2±0.52 (100)	5300±4500 (101)	0.50 (80)	0.53 (94)
19b	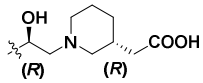	22±13 (100)	4500±2000 (95)	nt	nt

[a]EC_{50} values are shown as a mean of at least three determinations; [b]EC_{50} values are shown as a mean of two determinations

Table 5. SAR of 5-Substituted Trifluoromethyloxazole Ethanolamines

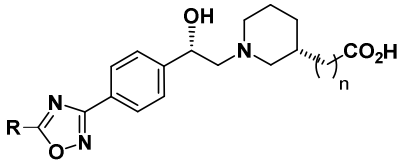

Compds	R	n	S1P$_1$ GTPγS EC$_{50}$, nM (Ymax)	S1P$_3$ GTPγS EC$_{50}$, nM (Ymax)	Rat BLR[d] % lymphocyte reduction, 24h (dose)
18a	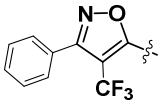	0	3.5±1.5[c] (98)	9400±5200[c] (87)	-54% (0.3 mpk)
19a		1	1.2±0.52[c] (106)	5300±4500[c] (101)	-80% (0.3 mpk)
20a	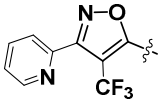	0	12[b] (98)	>31000[b]	-50% (5 mpk)
20b		1	2.4±1.3[c] (106)	14000±7200[c] (99)	-61% (0.3 mpk)
21a	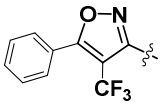	0	9.7[b] (97)	10000[c] (90)	-13% (1 mpk)
21b		1	3.9±1.0[c] (105)	4800[b] (100)	-76% (0.3 mpk)
22a	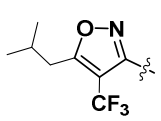	0	7.8[a] (104)	7400[a] (83)	-15% (1 mpk)
22b		1	2.3[b] (99)	1800±840[c] (74)	-6% (0.3 mpk)
23		1	1.1[a] (90)	2100[a] (119)	-49% (0.3 mpk)

[a]EC$_{50}$ values are shown as single determinations; [b]EC$_{50}$ values are shown as a mean of two determinations; [c]EC$_{50}$ values are shown as a mean of at least three determinations; [d]Compounds tested in Lewis rat (n = 3)

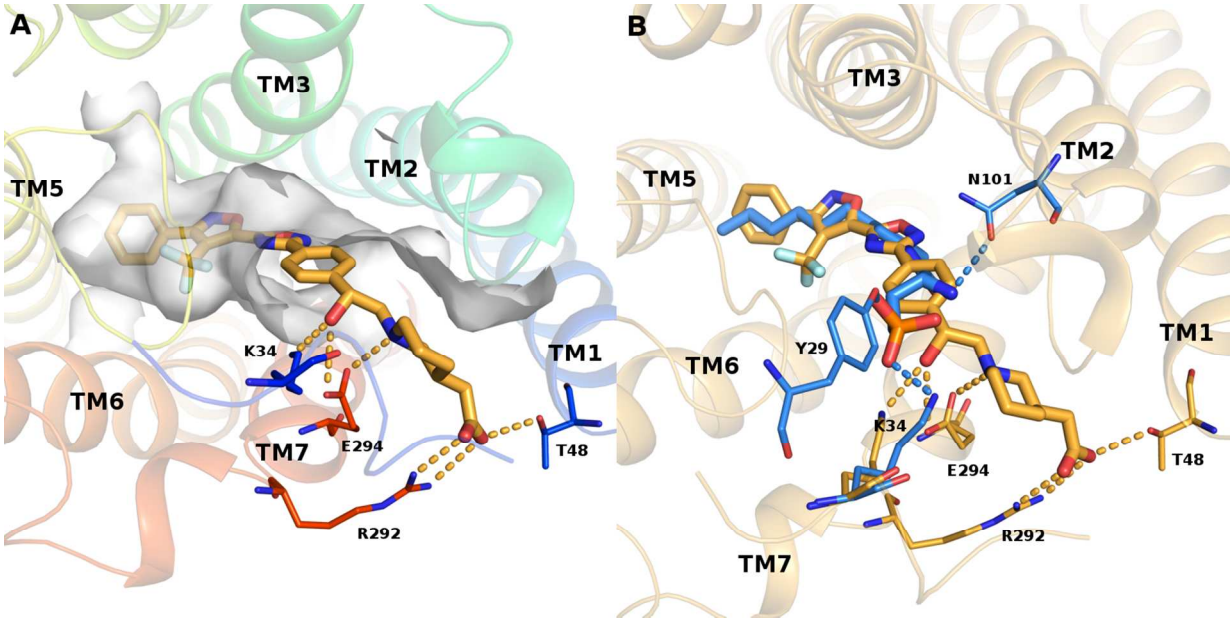

Figure 2. Predicted binding mode of compound **19a** in $S1P_1$. A) Docked conformation of compound **19a** in the $S1P_1$ crystal structure (PDB code 3V2W). The hydrophobic pocket is shown as a surface and the polar interactions as sticks. B) Overlay of the crystallographic ligand **24** (blue) and **19a** (orange).

Figure 3[a]**.** Dose Response of **18a** (0.1, 0.3, and 1.0 mg/kg) and **19a** (0.03, 0.1, and 0.3 mg/kg) *vs.* vehicle in the blood lymphocyte reduction assay in Lewis Rats.

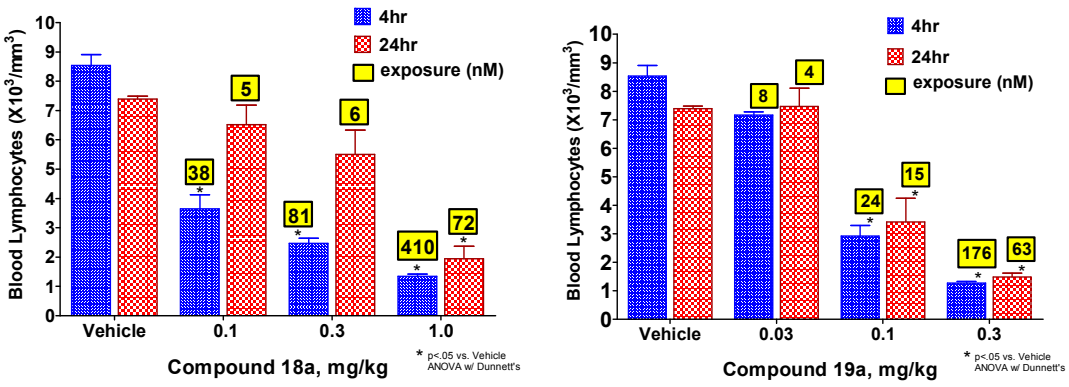

Table 6. Pharmacokinetic Parameters for Compound **18a and 19a**

species	Dose (mgKg)	Cmax ,μM (Tmax, h)	AUC (0-24h) (μM*h)	IV CL (L/min/kg)	Vss (L/kg)	IV $T_{1/2}$ (h)	F% (PO)	Peak/trough
Pharmacodynamic properties of 18a[a]								
mouse	IV: 1 PO: 1	45 (1)	362	0.1	0.1	15	66%	1.7
rat	IV: 2 PO: 5	5.3 (3.3)	60	1.7	1.2	9	76%	6.7
monkey	IV: 1 PO: 1	1.1 (4)	17	0.7	1.8	33	88%	1.7
dog	IV: 1 PO: 1	0.84 (0.8)	1.3	1.4	1.4	12	74%	11.3
Pharmacodynamic properties of 19a[a]								
mouse	IV: 1 PO: 1	44 (0.5)	315	0.1	0.2	23	62%	1.3
rat	IV: 2 PO: 5	4.7 (3.7)	66	1.0	2.2	28	87%	1.9
monkey	IV: 1 PO: 1	1.5 (10)	26	0.5	1.1	27	90%	2.7
dog	IV: 0.5 PO: 0.5	489 (4)	7.8	1.3	1.8	24	90%	2.8

[a] F = bioavailability; C_{max} = maximal concentration reached in plasma; T_{max} = time at which C_{max} was reached; Cl = clearance, Vss = volume of distribution at steady state

.

Figure 4[a]**.** Efficacy of **19a** (0.06, 0.2, and 1.0 mg/kg) *vs.* vehicle in a Rat Adjuvant Arthritis model.

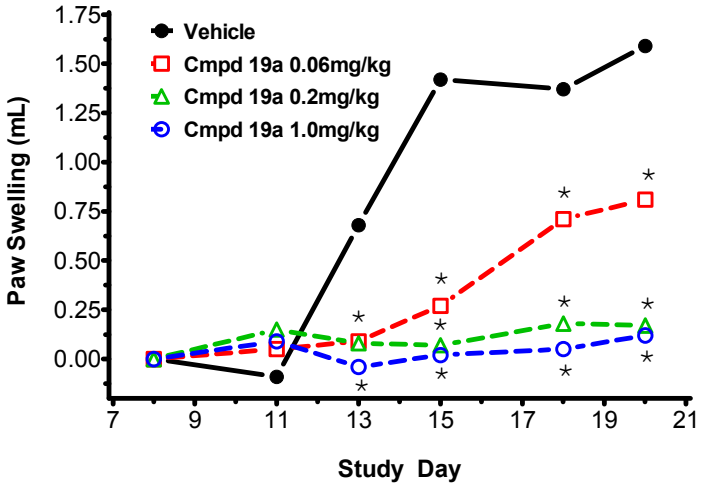

[a]Rats (n=8/group) were administered **19a** PO/QD starting on Day 0 at the time of immunization. Vehicle: PEG300.
*p value < 0.05 compared to vehicle treatment group.

Figure 5[a]. Efficacy of **19a** (0.01, 0.1, and 1.0 mg/kg) and *vs.* vehicle in a Mouse experimental autoimmune encephalomyelitis model (EAE).

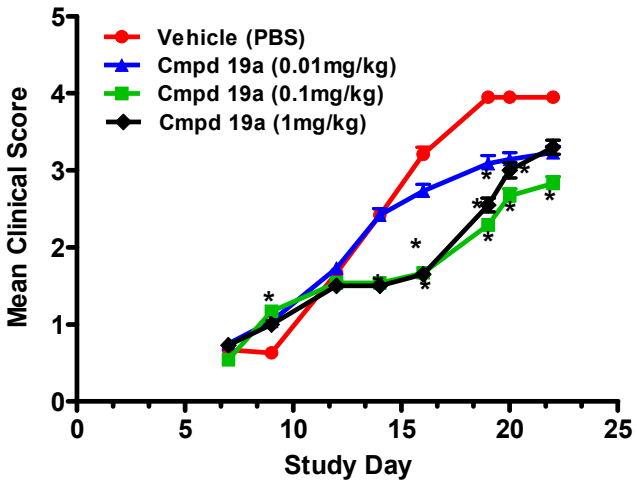

[a]Mice (n=10/group) were administered **19a** PO/QD starting on Day 0 at the time of immunization with MOG-peptide (myelin oligodendrocyte glycoprotein). Vehicle: PEG300. *p value < 0.05 compared to vehicle treatment group.

Table 7. *In vitro* profiling data for Compound **19a**.

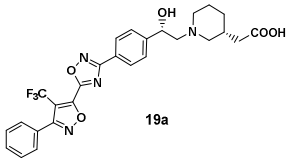

19a

Parameter	Result
Protein Binding (% bound)	<99.0% human
	99.8% mounse
	99.5% rat
	99.3% dog
	99.1% monkey
Mutagenicity	Ames negative
hERG (Patch Clamp)	IC_{50} = 4.1 μM[a]
Na^+ (Patch Clamp)	14% @ 10 μM (1 and 4 Hz)
Ca^+ (Patch Clamp)	14% @ 10 μM
CYP[a] inhibition (IC_{50})	>40 μM 1A2, 2B6, 2C9, 2C19,
	2D6, 3A4; 2C8 = 22 μM
Aqueous Solubility	>850 ug/mL (pH 1)
	229 ug/mL (pH 6.5)
PAMPA[b] permeability	295 nm/s @ pH 7.4
pKa	8.8
Log D (pH 6.5)	3.94

[a] Average of 3 replicates; [b]Cyp = cytochrome P450; [b]PAMPA = parallel artificial membrane permeability assay

TOC Graphic

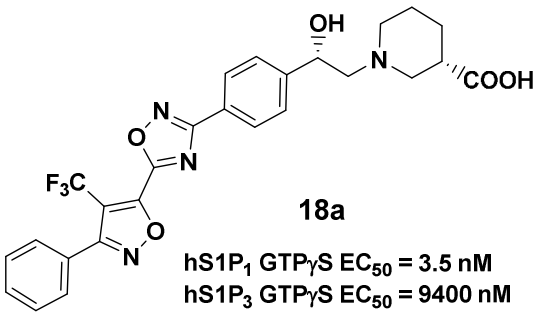

18a

$hS1P_1$ GTPγS EC_{50} = 3.5 nM
$hS1P_3$ GTPγS EC_{50} = 9400 nM
BLR PK/PD ED_{50} = 0.6 mpk

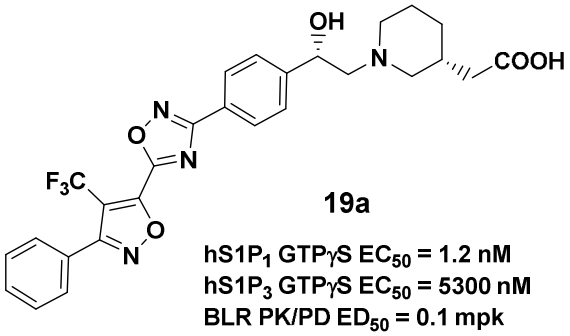

19a

$hS1P_1$ GTPγS EC_{50} = 1.2 nM
$hS1P_3$ GTPγS EC_{50} = 5300 nM
BLR PK/PD ED_{50} = 0.1 mpk